VISIBLE LIGHT PHOTOCATALYSIS WITH SUPPORTED METAL NANOPARTICLES FOR ORGANIC SYNTHESIS

Fan Wang

(n9221671)

Bachelor of Science (Chemistry)

Thesis completed under supervision of Prof. Huaiyong Zhu and Prof. Eric Waclawik, submitted to Queensland University of Technology, in fulfilment of the requirements for the degree of Master of Applied Science

School of Chemistry, Physics and Mechanical Engineering

Science and Engineering Faculty

Queensland University of Technology

2016

Keywords

Photocatalyst; Visible light; Localized surface plasmon resonance; Plasmonic photocatalyst;

Nonplasmonic photocatalyst; Gold nanoparticles; Alloy nanoparticles; Organic synthesis

Abstract

Photocatalysis, utilizing solar energy to drive chemical transformation attracts dramatically increasing interest nowadays. The main advantages of photocatalysis compared to the traditional thermal catalytic process are 1) efficiently apply light – the reliable, green and abundant energy source; 2) drive chemical reactions under very mild conditions – ambient temperature and atmospheric pressure; 3) restrain the yield of undesired by-product and thus achieve higher product selectivity due to the moderate reaction condition. Nanoparticles (NPs) of plasmonic metals such as gold (Au), silver (Ag) and copper (Cu) emerged as a class of new photocatalysts due to 1) strong light absorption of both visible light and UV light, and 2) high affinity with organic molecules. This project aims to develop a new series plasmonic metal-based photocatalysts that can exhibit high activity and selectivity for organic reactions under visible light irradiation at moderate temperature.

Localized surface plasmon resonance (LSPR) effect on the classic plasmonic metals: Au, Ag, Cu, and the influential factors of the LSPR absorption is introduced, followed by the optical and photocatalytic property introduction of rarely reported nonplasmonic transition metal NPs photocatalysts such as palladium (Pd), platinum (Pt), rhodium (Rh). The application of plasmonic-metals and nonplasmonic metals in photocatalytic process are also included to illustrate their performance and light absorption mechanism.

My first project is to design high effective supported Pd NPs on zirconium oxide (ZrO_2) to drive the well-known Heck reaction under light irradiation. After optimized reaction conditions, we found that this heterogeneous catalyst with 1.0 wt% Pd loading achieved high activity and selectivity as well as exhibited well tolerance of various Heck aryl halides and olefins substrates at atmospheric pressure and ambient temperature. The photocatalytic

performance was affected by several factors such as, solvent, base, reaction temperature, light intensity and wavelength. Furthermore, tuning the light intensity and wavelength of irradiation can manipulate the isomerization of cross-coupling product. Evidently, an effective and potential protocol is described and the results offer an alternative green route for more cross-coupling reaction, and open a new door for more nonplasmonic transition metals contributing in more organic reactions not only as the thermal activated catalysts but also with their photocatalytic capabilities.

In the second project, I attempted to apply supported Au NPs in thermal reaction and described that the supported Au NPs on ZrO_2 can be used as an efficient catalyst for the self-esterification of aliphatic alcohols to corresponding aliphatic esters under mild conditions. This heterogeneous catalyst achieved high activity and selectivity in a wide range of less reactive straight-chain alcohols (C_4-C_{12}) at green atmospheric pressure molecular O_2 and ambient temperature (45 ℃). After tested a series of catalysts with different Au content, it is found that the Au loading with 3.0 wt% achieved highest catalytic activity and selectivity. The AuNP catalysts are also efficient and readily recyclable. The finding of this study may stimulate further exploration on new catalytic systems for expansive organic syntheses using supported AuNP catalysts.

Overall, the discovery of these new metal NPs catalysts in organic synthesis reveals new mechanisms for the controlled transformation of chemical synthesis both in thermal environment and under visible light. The results of this project may inspire further studies on other efficient photocatalyst and enhance the potential to utilize sunlight via a more controlled process.

List of Abbreviations

Au	Gold
Ag	Silver
Cu	Copper
Pd	Palladium
NPs	Nanoparticles
LSPR	Localized Surface Plasmon Resonance
SEM	Scanning Electron Microscopy
TEM	Transmission Electron Microscopy
UV	Ultraviolet
UV-Vis	Ultraviolet Visible
XPS	X-ray Photoelectron Spectroscopy
XRD	X-ray Diffraction
EDX	Energy Dispersive X-ray Spectroscopy
TON	Turnover Number
TOF	Turnover Frequency

Statement of Original Authorship

The work contained in this thesis has not been previously submitted to meet requirements for an award at this or any other higher education institution. To the best of my knowledge and belief, the thesis contains no material previously published or written by another person except where due reference is made.

Signature: QUT Verified Signature

Date: 12 / 08 / 2016

Acknowledgements

I would like to deliver my thanks to all those who have helped and supported me throughout the period of my master career.

Firstly, I would like to express my sincere gratitude and appreciation to my principal supervisor Prof. Huaiyong Zhu and associate supervisor Prof. Eric Waclawik, for giving me guidance, inspiration, caring, valuable scientific knowledge and research experiences.

Secondly, great acknowledgements are to my senior colleague Dr. Qi Xiao and Dr. Sarina, for the valuable suggestions and professional teach on my research.

My sincere appreciations also extend to Dr. Lauren Butler, Leonora Newby and other technicians who have provided assistance at instruments technology. Great thanks to Mr. Tony Raftery for his training and assistance of XRD.

Special thanks, of course, go to my dear colleagues: Yiming Huang, Gallage Sunari Peiris, Pengfei Han, Arixin Bo, Zhe Liu and Xiayan Wu who assisted me and provide convenience to me in conducting the lab work.

Table of Contents

Chapter 1:

Introduction and Literature Review

1.1 Introduction

Nowadays, the development of industry has caused excessive energy demand and that is exhausting fossil fuel supply at an astonishing speed and increasing global carbon dioxide (CO_2) emission at an alarming rate. In other words, traditional chemical industry brings severe pollution to environment. In 1991's, the US Environmental Protection Agency (EPA) proposed the term "Green Chemistry" which advocates the clean industry processes to eliminate waste.[1] Ever since then, the developments in Green Chemistry have gained extensive attention. Under such background, it is urgent and necessary to find alternative way to replace the traditional production mode, which is ideal to develop environmental technologies and transformations that are driven by clean renewable energy sources. In numerous choices, natural sunlight, an abundant, clean and renewable resource, stands out the most promising candidate to meet our society requirement. It is public known that the earth received 3×10^{24} joules energy every year from sun, which is approximately 10,000 times than the global population consumes currently. Thus, a reasonable hypothesis can be proposed: if we even exploit 0.01% of the solar energy, we can effortless solve the problem of energy shortage and reusable. Applying the light energy to drive chemical reactions is known as photochemistry, and photochemistry along with life as we know it originated on earth billions of years ago.[2] Utilizing light could shift apparent thermodynamic emphasis from performing high-temperature to favor room temperature chemical synthesis, which thus

restrain the unwanted side products.[3] In additional, the use of solar energy instead non-reusable energy can not only alleviates energy shortage but also in favor of environment protection. Various organic reactions are synthesized via thermal process and often require harsh reaction conditions such as high temperature and pressure, which significantly increased the reaction efficiency. Meanwhile, it results in huge damage to our environment and substantial amount of by-products are generated. Therefore, it is a significant breakthrough if we can conduct important organic reaction in moderate condition meanwhile using one kind of cheaper, abundant and greener energy source to minimize the environmental and economical impacts of chemical processes. In summary, photocatalysis is fascinating in the area of green chemistry as it achieves the high efficiency of catalysis by utilizing renewable resource – sunlight under moderate condition.[4-6]

1.2 Literature Review

1.2.1 Plasmonic-Metal Nanoparticles

Plasmonic is a study focus on the interaction between electromagnetic field and free electrons in a metal. Since 1990s, medieval artisans used micro and nano-scale pieces of metal embedded in glass to make the vibrant colors in stained glass windows and ornamental pieces. Nano-scale pieces of metal reflect light differently to bulk pieces of metal. The nano-scale pieces of metal have resonances and this resonance of the metal nanostructure is known as a plasmon. Nowadays, plasmonic-metal nanoparticles (NPs) are considered as a novel medium rely on their strong interaction with a wide range of light region through excitation of the localized surface plasmon resonance (LSPR).[7-9] LSPR is the resonant collective oscillation of valence electrons of metal, and occurs when the incoming light wavelength far larger than the nanoparticles diameter as well as the incident photon frequency matches the intrinsic frequency of metal surface electrons oscillating against the restoring force of positive nuclei (Figure 1).
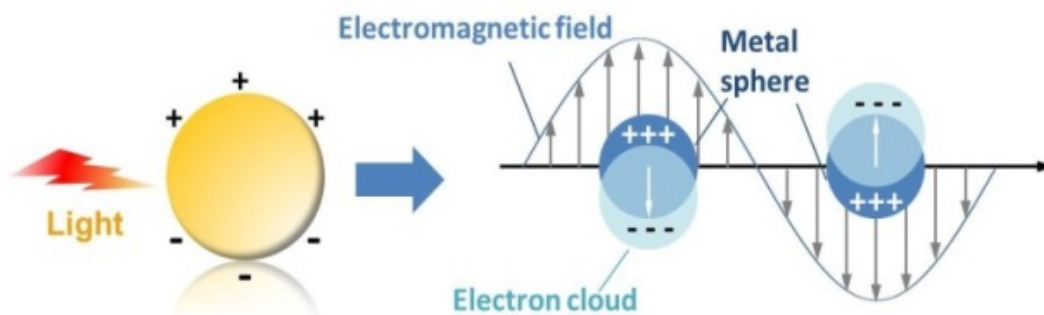
Figure 1. Localized surface plasmons resonance (LSPR) effect of a metal nanosphere.[10]

This kind of optical properties are dominated by several factors – the dielectric constants of the metal and its surrounding material, the particle size and the particle shape. The intrinsic dielectric properties of the metal and its surrounding medium and the surface polarization can affect the frequency and strength of the plasmon resonance, which primarily determined by particle size and shape as any change of them can tailor the surface polarization results a change to the plasmon resonance.[11-14] Ag NPs is a characteristic of this shape and size determined property. Figure 2 shows the discrete dipole approximation (DDA) calculated extinction, adsorption and scattering spectra of 40 nm Ag NPs of various shapes suspended in water.
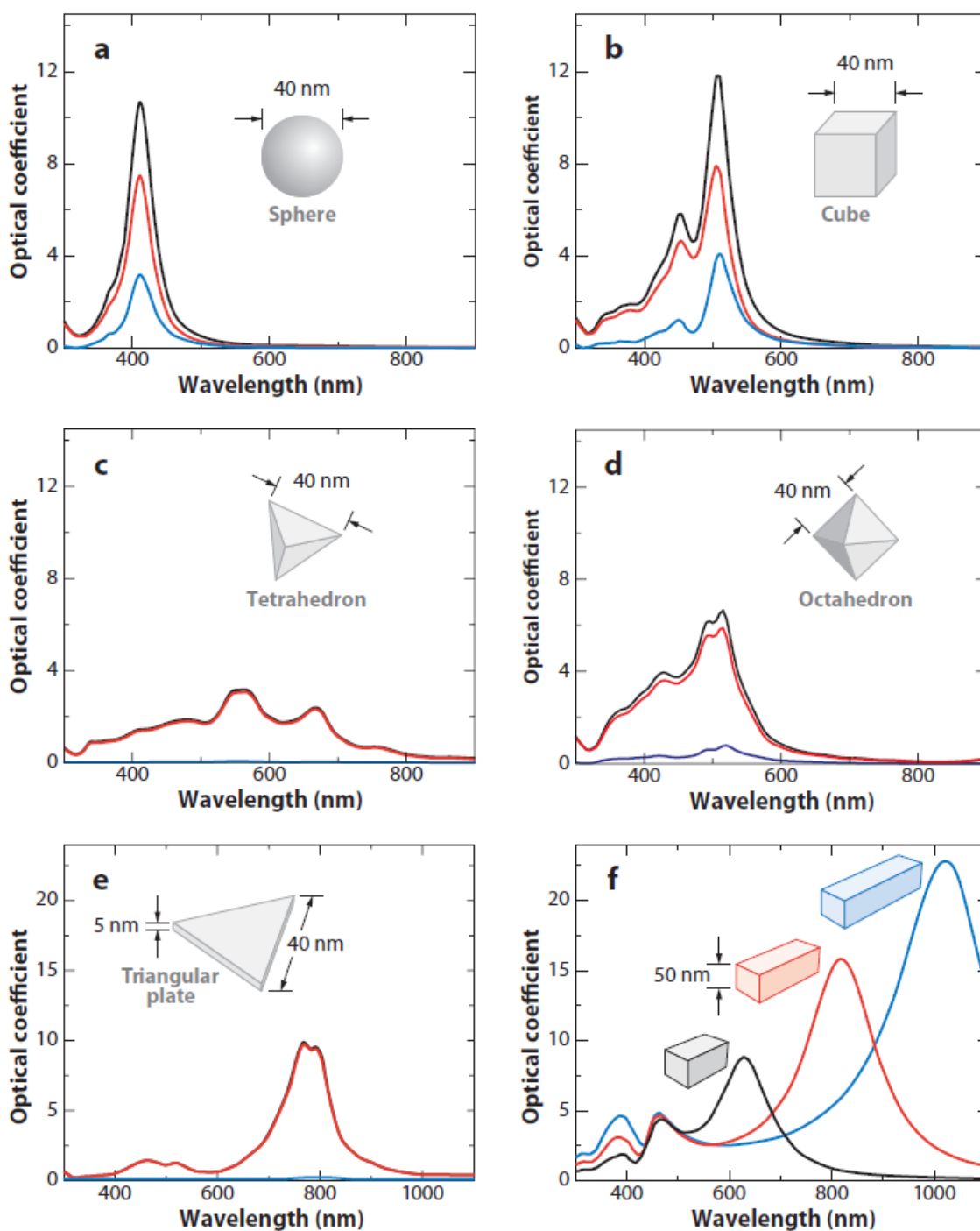
Figure 2. Calculated UV/Vis extinction (black), absorption (red), and scattering spectra (blue) of Ag nanocrystals, which illustrates the effect of NP shape on spectral characteristics: a) sphere, b) cube, c) tetrahedron, d) octahedron, e) triangular plate, and f) rectangular bars with aspect ratios of 2 (gray), 3 (red), and 4 (blue).[10]

Comparing to the Ag nanosphere (Figure 2a), the most intense peak position of Ag nanotube (Figure 2b) is red-shift compared with that of the nanosphere, which indicated that resonance peaks redshift with increasing sharpness corner and particle anisotropy. All the tetrahedron, octahedron and even two-dimensional Ag triangular plate shape show further red-shift of LSPR peaks since they have sharper corners than cubes (Figure 2c, 2d and 2e). That means the particle symmetry resulted in the LSPR peak intensity increased.

The noble metal NPs utilizing the LSPR effect has been recognized as a new way for utilizing light energy to drive chemical processes due to their high optical absorption. The conventional and classic noble metal NPs are Au, Ag and Cu. As shown in Figure 3, the typical plasmon resonance band (SPB) for colloidal aqueous noble metal NPs indicated that the LSPR absorbance of Au, Ag, and Cu are all within the visible region. Au, Ag and Cu spherical NPs exhibited maximum at $\lambda \approx$530, 400 and 580 nm, respectively. All the combined information suggests that palsmonic NPs are enable for direct photocatlysis.
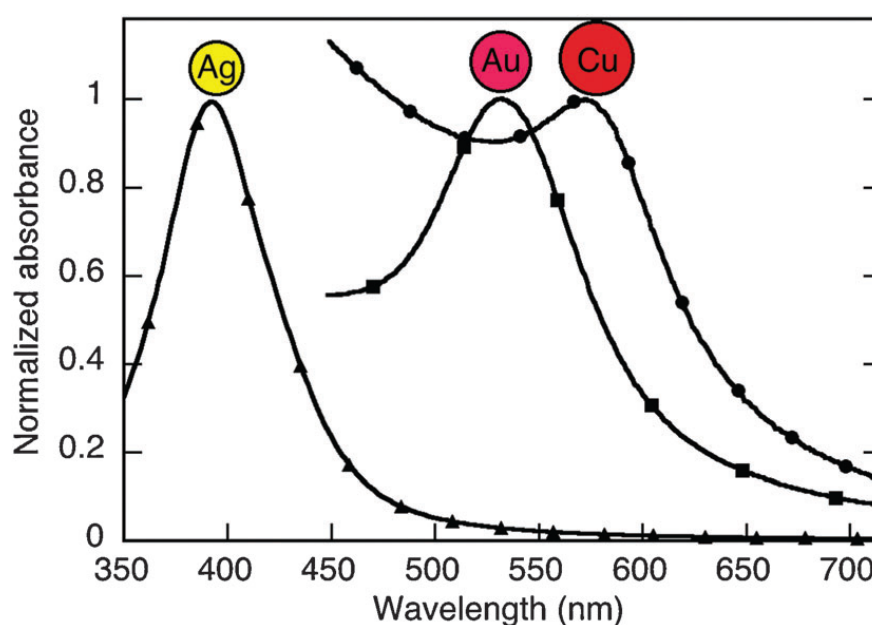

Figure 3. Surface plasmon absorption bands for Au, Ag, and Cu NPs.[15]

Our group had reported that the supported Au NPs can catalyze the colatile organic compounds (VOCs) oxidation under light irradiation.[16] It was the first experimental

observation of plasmonic NPs direct-driven in photocatalysis reaction. Since then, direct photocatalysis with plasmonic metal NPs was applied in many reaction systems. The mechanism can be generally described as charge-carrier-driven reaction which is summarized by Linic et al. recently.[17] To sum up, chemical reaction on metal surface can be achieved by light stimulus. In this situation, once reactant has been absorbed on metal surface, external light can excite charge-carriers (electrons and/or holes) results in energized charge-carriers (excited state), then thus inducing the activation of chemical bonds and chemical transformations.[18] According to the summarized by Christopher et al., there are three ways that the light energy can through to transfer directly into the reactants absorbed on plasmonic metal surface: 1) elastic radiative reemission of photons, 2) nonradiative Landau damping, resulting in the excitation of energetic electrons and holes in the metal particle, and 3) the interaction of excited surface plasmons with unpopulated adsorbate acceptor states, inducing direct electron injection into the adsorbate acceptor states, called chemical interface damping (CID, Figure 4).[19]
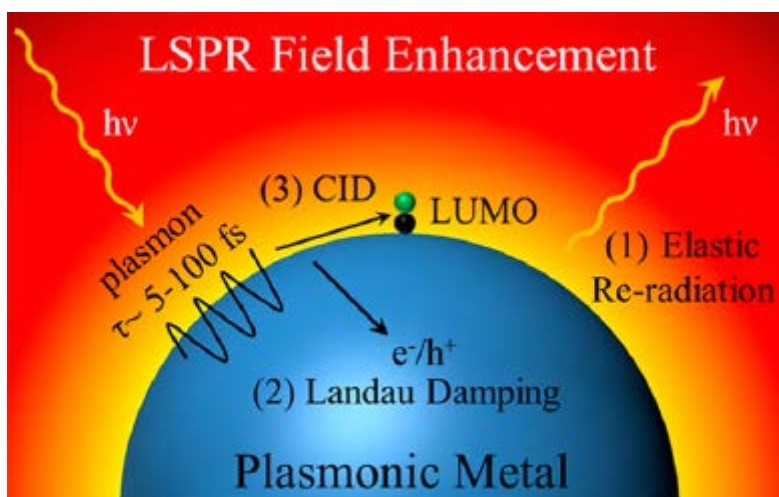

Figure 4. Schematic showing the three dephasing mechanisms of oscillating surface plasmons.[19]

1.2.2 Nonplasmonic-Metal Nanoparticles

Unlike plasmonic-metal NPs, nonplasmonic-metal NPs are rarely reported about their photocatalytic capabilities, but are common known as their thermally activated catalysts for various important organic reaction.[20] The most difference between plasmonic-metal NPs and nonplasmonic-metal NPs is the process of utilizing light energy. Plasmonic-metal NPs utilizing LSPR effect to absorb light energy, however, nonplasmonic-metal NPs, such as palladium (Pd), platinum (Pt), rhodium (Rh) and iridium (Ir), strongly absorb the light mainly through interband electronic transitions. Figure 5 shows the light-absorption spectra of Pd, Pt, Rh and Ir. The light absorption of pure ZrO_2 is also included and it exhibited negligible light absorption in the UV-Visible region.
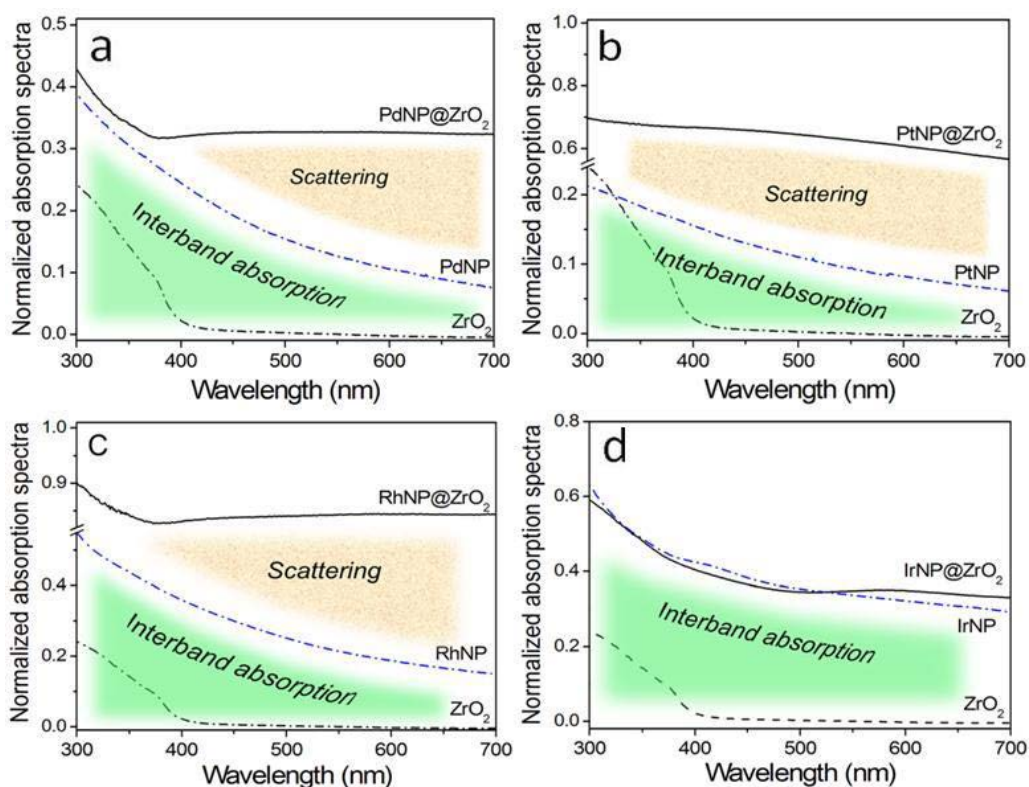

Figure 5. Light absorption spectra of the metal nanoparticles in a colloid suspension (dash line) and supported on ZrO_2 (solid line). a) Pd NPs, b) Pt NPs, c) Rh NPs, d) Ir NPs.[21]

According to this figure, we can conclude that light absorption of Pd, Pt, Rh and Ir supported on ZrO_2 in the UV-Visible spectra mainly due to the absorption of the nonplasmonic-metal NPs, which ascribe to the interband contribution.

1.2.3 Supports materials

1.2.3.1   Semiconductor

It is feasible for plasmonic NPs directly catalyzing organic reaction under visible light irradiation without any support. However, they are not stable under normal photocatalytic reaction conditions.[3] In this situation, most plasmonic NPs catalysts are supported on a solid inert support in practical photocatalysis process. Furthermore, as heterogeneous catalysts, supported plasmonic NPs are easily separated from the solution after reaction. In these system, semiconductor are widely used for various chemical transformations induced visible or UV light such as splitting of water, the degradation of VOCs and the dye-sensitized solar cells.[22-24] An electron transformation mechanism can be utilized to explain the photoelectrochemical response.[25] Semiconductor only can absorb photons with energy greater than or equal to their bang-gap energy. As show in Figure 6, when the semiconductor is exposed under irradiance, the incoming photons excited electrons from the valence band to the conduction band, meanwhile leaving positively charged holes in the valence band and then migrate to the particle surface to reduce and oxidize species absorbed on the solid surface.
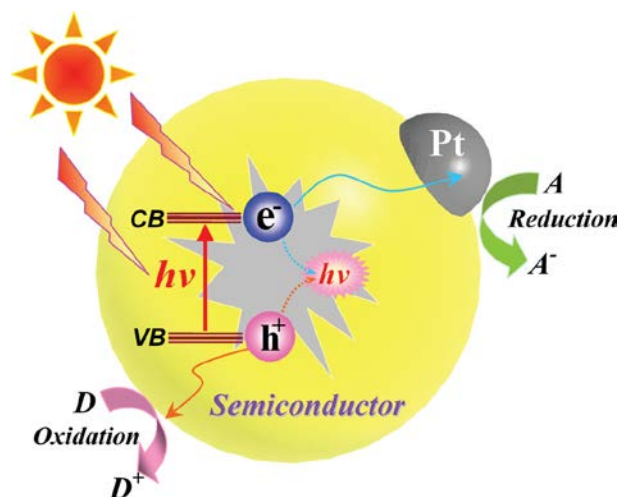
Figure 6. Mechanism of semiconductor photocatalysis process.[26]

There are mainly two aspects for semiconductors which should be considered: a) wide band-gap and b) weak affinity toward organic adsorbates. For the former aspect, whether the band gaps are too wide or too narrow, they are both unstable for practical use.[27] For example, semiconductor TiO_2 is a promising material widely used as support since Fujishima and Honda discovered the water splitting on TiO_2 electrode in 1972.[28] However, the band gap of TiO_2 is 3-3.2 eV and due to its wide bang gap, it can only utilize ultraviolet (UV) radiation which accounts only a small fraction (no more than 5%) of the whole incoming solar energy. In order to maximum utilizing the solar energy, narrowing the bang gap of such semiconductor by experimental method is a priority choice. Various approaches have been developed this years including doping metal ions or metal atom cluster,[29,27] integrating nitrogen[30] and applying other metal oxides as catalyst materials.[31,32] For another aspect, some semiconductor possess weak affinity toward various organic reactant and low surface concentrations of active sites for catalyzing the reactions. Due to the intrinsic limitation of semiconductor, the absorption of light and efficiency of photon are influenced significantly. Searching new materials that can work under the full sunlight spectrum is still necessary and significant.

1.2.3.2   Insulator

The insulator is a kind of materials that its internal electric charges do not flow freely, thus cause it almost impossible to conduct electric current under the influence of the electric field. Furthermore, since the band gap (between the valence band and the conduction band) of insulator is larger than semiconductor, the free electrons in the valence band are not able to be exited to the conduction band even are irradiated under UV light. In this case, photocatalytic activity of insulator photocatalysts is determined only by two factors: a) the electromagnetic field of neighbouring NPs and b) the direct interaction of the LSPR excited energetic electrons with reactants.

When the NPs are irradiated by the incoming photons, LSPR is able to collect the light energy into a limited volume around the nanostructures, thus enhancing the electric field intensity. We define the area between this high-intensity fields and plasmonic NPs as hot spots which represent a significant one in photocatalysis.[33] Our group has applied ZrO_2 supported Au NPs in many organic reaction under light irradiation.[16,34-36] According to our investigation, we found that the conduction gain the energy of incoming photons through LSPR absorption and interband absorption. The resulted energetic electrons at Au NPs surface can interact directly with reactant and activated subsequently in chemical reaction.

1.2.4 Important Influential factors in photocatalysis

1.2.4.1   Light intensity

The photocatalysis rates highly depend on light intensity as it determines the photon flux. It is well-known that there exists a positive relationship between quantum efficiency and photon flux. Therefore, a stronger light intensity resulted in higher quantum efficiency. Figure 7 shows the light intensity dependence of photocatalytic activity using the Au NPs for conversion of benzyl alcohol.
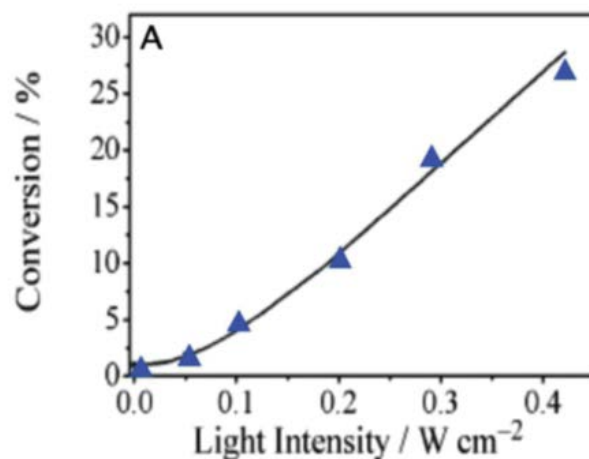
Figure 7. The effect of the light intensity on benzyl alcohol oxidation under visible light catalyzed by Au/zeolite.[37]

When the light intensity increased from 0.1 to 0.4 W/cm^2, the relationship between light intensity and conversion rate exhibited almost linear. In this reaction, the stronger light intensity excited more energetic electrons of Au NPs with sufficient energy to drive the reactions. Thus, the conversion increases with the raising of light intensity. The results also demonstrated that light intensity played a significant role in photocatalytic reaction.

1.2.4.2   Wavelength

The wavelength of incident light dominating the photocatalytic activity is another characteristic of plasmonic metal NPs. There is different mechanisms and explanation of semiconductor and plasmonic NPs photocatalysts absorbing light with different wavelength. For semiconductor photocatalysts, the wavelength of light should short enough at least can produce photons with sufficient energy higher than the band gap of semiconductor. In the other word, the possibility of charges generation of incoming light inducing photocatalytic reaction is fixed no matter how the wavelength of the irradiation altered. On the other hand, the electron excitation of metal NPs under light irradiation with various wavelengths also has different mechanism and explanation. It has been demonstrated that LSPR is highly related to

the observed photocatalytic activity. A useful tool to clarify the relationship between photocatalytic rate and wavelength of light is the action spectrum (the rate of reaction activity plotted against wavelength of light).[38,39] It is able to reflect the coincidence of the wavelength-dependent photocatalytic rate and the light absorption spectrum. Our group once conducted the reduction of nitrobenzene under light irradiation by using Ag-Cu(4-1)@ZrO$_2$ photocatalyst,[40] and the action spectrum of this reaction is presented in Figure 8.
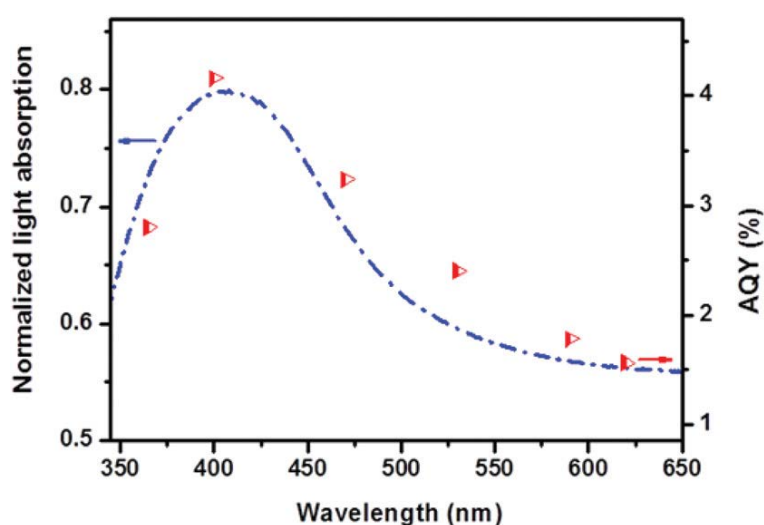
Figure 8. Photocatalytic action spectrum for the reduction of nitrobenzene using Ag-Cu(4-1)@ZrO$_2$ photocatalyst.[40]

The trend of AQY (red triangles) well matches with the light absorption curve of the Ag-Cu alloy NPs photocatalyst, and described the relationship between the action spectrum and the plasmon intensity. That suggesting the excitation of light with different wavelength is responsible for the obtained photocatalytic activity.

1.2.5 Application of Metal Nanoparticles Photocatalysts.

The noble metal NPs photocatalysts are able to driving chemical reactions through LSPR effect in an efficient way by utilizing visible light. Here we introduced some application of them.

1.2.5.1 Reaction catalyzed by Nobel Metal Photocatalysts

Investigation of optical property and catalytic ability of the noble metal NPs has never declined since it was first time found that Au NPs is capable catalyzed the degradation of volatile organic compound at mild condition under visible light irradiation.[16] We will focus on both insulator and semiconductor supported Au NPs in photocatalytic reaction.

(1) Semiconductor supported Au (Au/TiO$_2$) photocatalytic reaction.

In 2010, Zheng et al. reported four types of TiO$_2$ nanostructure all supported Au NPs were applied in the oxidation of formaldehyde (HCHO) under visible light irradiation.[25] All of the four different types of Au/TiO$_2$ photocatalysts exhibited significant activity.
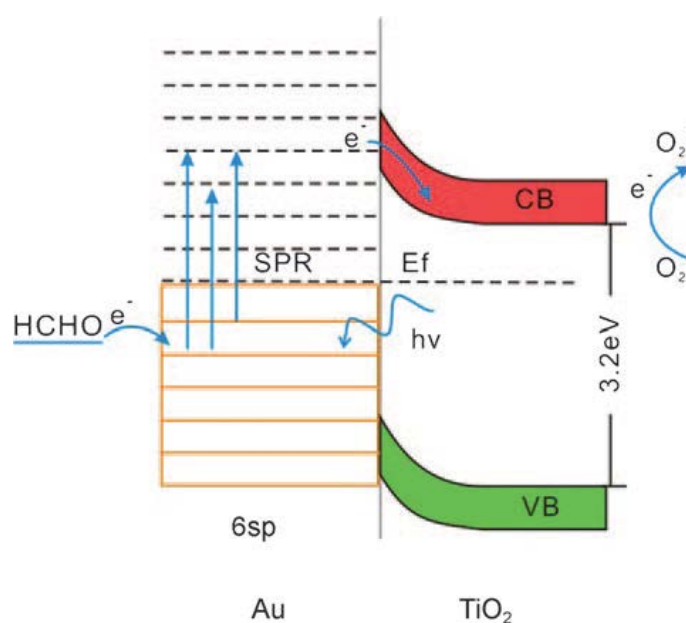
Figure 9. Energy diagram of Au/TiO$_2$ catalysts showing the oxidation of HCHO by the SPR effect of Au NPs under visible light.[43]

Although even change the semiconductor support TiO$_2$ to other insulator like ZrO$_2$ or CeO$_2$, Au NPs are also able to exhibit high activity,[16] however, the mechanism between them is totally different. In the presented work, visible light are capable of excited the electrons of Au NPs from 6 sp to higher level and then migrate to the TiO$_2$ conduction band, meanwhile

leaving positive charges on the Au NPs. The Au NPs can receive electrons from HCHO absorbed on them (Figure 9).

(2) Insulator supported Au (Au/ZrO$_2$) photocatalytic reaction.

For Au NPs supported on insulator as photocatlyst, our group have prepared Au NPs on ZrO$_2$ with 3 wt% of overall catalyst mass (Au/ZrO$_2$ 3 wt%) and found that it exhibited excellent activity for the reduction nitro-aromatic compounds to azo compounds under UV and visible light at mild conditions (Equation 1).[36] The nitrobenzene was completely reduced to the product with more than 99% azobenzene within 5 hours.

$$\text{PhNO}_2 \xrightarrow[\text{hv, 40 °C, 1 atm Ar}]{\text{Au/ZrO}_2} \text{Ph-N=N-Ph} \qquad (1)$$
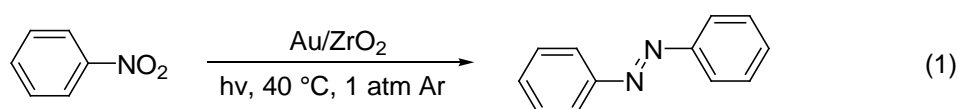
Conventionally, aromatic azo compounds were synthesized through a two-step, one-pot thermal reaction. Our report was the first protocol of directly reduction of nitro-aromatic compounds to azo compounds in moderate conditions, which is different from the condition of thermally catalyzed reaction. The reaction, utilizing visible light and catalyzed by supported Au NPs, is greener than thermal processes as it possesses the potential to utilize solar energy, which can be developed in expansive similar synthesis.

1.2.5.2 Reaction catalyzed by Alloy Nanoparticles Photocatalysts

The combination of one nonplasmonic metal (Pd) NPs and one plasmonic metal (Au) NPs supported on ZrO$_2$ (Au-Pd@ ZrO$_2$) exhibited superior activity at mild condition under light irradiation than any of the Au or Pd monometal NPs photocatalysts in various chemical reactions. For example, the Suzuki-Miyaura cross-coupling reactions and selective oxidation of aromatic alcohols to corresponding aldehydes, ketones and phenol oxidation.[41] The corresponding blank reaction were also conducted in the dark but keep other reaction condition identical, and all of them exhibited inert catalytic activity. As the large band gap of

ZrO$_2$ (5.0 eV), the ZrO$_2$ support contribute nothing to photocatalytic activity. The intrinsic catalytic activity of Pd NPs is highly enhanced by incorporating Au NPs, and the light absorption peak is also shifted and became broadest. (Figure 10.)
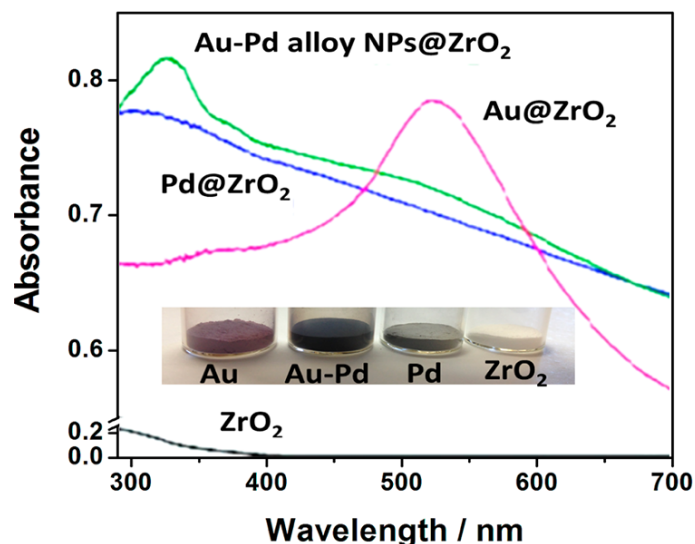

Figure 10. Diffuse reflectance UV−visible (DR-UV−vis) spectra of the Au−Pd@ZrO$_2$ catalyst and their comparison with pure Au@ZrO$_2$ and Pd@ZrO$_2$.[41]

Given that the electronegativity of Pd and Au is different (Pd 2.20, Au 2.54), there exists a charge heterogeneity on the alloy surface. Due to this property, interactions between the alloy NPs and reactant molecules can be enhanced,[42,43] and it acts a pivotal step in these photocatalytic reactions.

1.3 Summary

This chapter briefly reviews the development of photocatalysts and photocatalytic process, including the fundamental concept and mechanism of different photocatalysys and their performance under light irradiation. The direct plasmonic photocatalysts exhibited excellent catalytic activity under light irradiation mild conditions, which is more effectively and environmental friendly than the thermally driven catalysis. Furthermore, we should continue

to research other influence factors of the LSPR light absorption, such as particle size and shape and photothermal effect, which can provide with more controllable methods.

To sum up, study on the noble metal NPs to enhance the reaction rate by light irradiation is of great significance. Utilizing LSPR effect of metal NPs in photocatalysis provides the opportunity to achieve more chemical transformation more economical and utilize solar energy efficiently.

Reference list

1. D. Ravelli, D. Dondi, M. Fagnoni and A. Albini, *Chem. Soc. Rev.,* 2009, **38,** 1999–2011.

2. V. Ramamurthy, *Acc. Chem. Res.,* 2015, **48,** 2904−2917.

3. X. Lang, X. D. Chen and J. C. Zhao, *Chem. Soc. Rev.,* 2014, **43,** 473–486.

4. G. Palmisano, V. Augugliaro, M. Palmisano and L. Palmisano, *Chem. Commun.,* 2007, 3425–3437.

5. M. Fagnoni, D. Dondi, D. Ravelli and A. Albini, *Chem. Rev.,* 2007, **107,** 2725–2756.

6. S. Navalon, R. Martin, M. Alvaro and H. Garcia, *ChemSusChem,* 2011, **4,** 650–657.

7. P. V. Kamat, *J. Phys. Chem. B,* 2002, **106,** 7729–7744.

8. L. F. Qiao, D. Wang, L. J. Zuo, Y. Q. Ye, J. Qian, H. Z. Chen and S. He, *Appl. Energy,* 2011, **88,** 848–852.

9. S. Linic, P. Christopher and D. B. Ingram, Nat. *Mater.,* 2011, **10,** 911–921.

10. X. M. Lu, M. Rycenga, S. E. Skrabalak, B. Wiley and Y. N. Xia, *Annu. Rev. Phys. Chem.,* 2009, **60,** 167–192.

11. M. A. El-Sayed, *Acc. Chem. Res.,* 2001, **34,** 257–264.

12. C. Burda, X. B. Chen, R. Narayanan and M. A. El-Sayed, *Chem. Rev.,* 2005, **105,** 1025–1102.

13. K. L. Kelly, E. Coronado, L. L. Zhao and G. C. Schatz, *J. Phys. Chem. B,* 2003, **107,** 668–677.

14. L. Brus, *Acc. Chem. Res.,* 2008, **41,** 1742–1749.

15. J. C. Scaiano, K. G. Stamplecoskie and G. L. Hallett-Tapley, *Chem. Commun.,* 2012, **48,** 4798–4808.

16. X. Chen, H. Y. Zhu, J. C. Zhao, Z. F. Zheng and X. P. Gao, *Angew. Chem. Int. Ed.,* 2008, **120,** 5433–5436.

17. S. Linic, U. Aslam, C. Boerigter and M. Morabito, *Nat. Mater.,* 2015, **14,** 567–576.

18. J. W. Gadzuk, *J. Chem. Phys.,* 1983, **79,** 6341–6348.

19. M. J. Kale, T. Avanesian, and P. Christopher, *ACS Catal.,* 2014, **4,** 116–128.

20. D. Astruc, *Nanoparticles and Catalysis,* Vol. 1, Wiley-VCH, Weinheim, 2008, Chap. 1.

21. S. Sarina, H. Y. Zhu, Q. Xiao, E. Jaatinen, J. F. Jia, Y. M. Huang, Z. F. Zheng and H. S. *Wu. Angew. Chem. Int. Ed.,* 2014, **53,** 2935–2940.

22. T. Takata, A. Tanaka, M. Hara, J. N. Kondo and K. Domen, *Catal. Today,* 1998, **44,** 17–26.

23. M. Grätzel, *J. Photochem, Photobiol. C,* 2003, **4,** 145–153.

24. M. Kitano, K. Iyatani, K. Tsujimaru, M. Matsuoka, M. Takeuchi, M. Ueshima, J. M. Thomas and M. Anpo, *Top. Catal.,* 2008, **49,** 24–31.

25. Z. F. Zheng, J. Teo, X. Chen, H. W. Liu, Y. Yuan, E. R. Waclawik, Z. Y. Zhong and H. Y. Zhu, *Chem.–Eur. J.,* 2010, **16,** 1202–1204.

26. H. Tong, S. Ouyang, Y. Bi, N. Umezawa, M. Oshikiri and J. Ye, *Adv. Mater.*, 2012, **24**, 229–251.

27. W. Y. Teoh, R. Amal, L. Mädler and S. E. Pratsinis, *Catal. Today,* 2007, **120,** 203–209.

28. A. Fujishima and K. Honda, *Nature,* 1972, **238,** 37–38.

29. M. I. Litter, *Appl. Catal., B,* 1999, **23,** 89–114.

30. R. Asahi, T. Morikawa, T. Ohwaki, K. Aoki and Y. Taga, *Science,* 2001, **293,** 269–271.

31. S. Ikeda, M. Hara, J. N. Kondo, K. Domen, H. Takahashi, T. Okubo and M. Kakihana, *Chem. Mater.,* 1998, **10,** 72–77.

32. A. L. Linsebigler, G. Lu and J. T. Yates, *Chem. Rev.,* 1995, **95,** 735–758.

33. W. B. Hou, W. H. Hung, P. Pavaskar, A. Goeppert, M. Aykol and S. B. Cronin, *ACS Catal.,* 2011, **1,** 929–936.

34. H. Y. Zhu, X. Chen, Z. F. Zheng, X. B. Ke, E. Jaatinen, J. C. Zhao, C. Guo, T. F. Xie and D. J. Wang, *Chem. Commun.,* 2009, 7524–7526.

35. Y. B. Zhang, Y. N. Shen, X. Z. Yang, S. S. Sheng, T. N. Wang, M. F. Adebajo, and H. Y. Zhu, *J. Mol. Catal. A: Chem.,* 2010, **316,** 100–105.

36. H. Y. Zhu, X. B. Ke, X. Z. Yang, S. Sarina and H. W. Liu, *Angew. Chem. Int. Ed.,* 2010, **49,** 9657–9661.

37. X. G. Zhang, X. B. Ke and H. Y. Zhu, *Chem.–Eur. J.,* 2012, **18,** 8048–8056.

38. E. Kowalska, R. Abea and B. Ohtania, *Chem. Commun.,* 2009, **2,** 241–243.

39. A. Tanaka, S. Sakaguchi, K. Hashimoto and H. Kominami, *ACS Catal.,* 2013, **3,** 79–85.

40. Z. Liu, Y. M. Huang Q. Xiao and H. Y. Zhu, *Green Chem.,* 2016, **18,** 817–825.

41. S. Sarina, H. Y. Zhu, E. Jaatinen, Q. Xiao, H. W. Liu, J. F. Jia, C. Chen and J. Zhao, *J. Am. Chem. Soc.,* 2013, **135,** 5793−5801.

42. W. J. Tang and G. J. Henkelman, *Chem. Phys.,* 2009, **130,** 194504.

43. M. S. Chen, D. Kumar, C. W. Yi and D. W. Goodman, *Science,* 2005, **310,** 291−293.

Chapter 2:

Application of Supported Palladium Nanoparticles as Photocatalyst in Visible Light Irradiation

Introductory Remarks

In this charter, supported palladium nanoparticles (Pd NPs) was designed and applied for the Heck reactions in the irradiation of visible light in mild conditions. We prepared a range from 0.5 wt% to 5.0 wt% Pd nanoparticles supported on zirconium dioxide (ZrO_2) as photocatalyst. We found that supported Pd NPs showed sensitive activity of our reaction under light irradiation. For example, when the temperature was kept at 50 °C, there is no conversion in the dark supported 1.0 wt% Pd NPs as photocatalyst, while 100% conversion was achieved in the light irradiation at the same temperature. The conversion rate can be enhanced by strengthening light irradiation intensity and increasing the reaction temperature.

To better understand if the reaction occurs via a light-induced process, we conducted the action spectrum to show the relationship between light absorption and reaction rate. Furthermore, the altered of light intensity and wavelength can manipulate the isomerization of cross-coupling product. The highest selectivity of cis-stilbene was obtained when the light intensity reached highest (0.5 W/cm^2), and the selectivity increased with the increasing of light intensity and the decreasing of wavelength. The research on Pd NPs photocatalysts can

promote the study on nonplasmonic-metal photocatalysts and improve the application of sunlight to drive more chemical reactions.

Statement of Contribution of Co-Authors

Publication title and date of publication or status:

Photocatalytic Heck Cross-Coupling Reaction using Supported Palladium Nanoparticle as Catalysts

Fan Wang, Qi Xiao, Sarina Sarina and Huaiyong Zhu*

Manuscript submitted

Contributor	Statement of contribution
Student Author: Fan Wang Signature: Fan Date: 12/08/2016	Discovered the photocatalytic reaction, organized and designed the experiments, conducted the data collection, analyzed the data, proposed the reaction mechanism and wrote the manuscript
Qi Xiao	Analyzed data, offered interpretations, revised the manuscript
Sarina Sarina	Give constructive suggestion on the reaction
Prof. Huaiyong Zhu	Proposed the idea and polished the manuscript

Principal Supervisor Confirmation

I have sighted email or other correspondence from all Co-author confirming their certifying authorship.

Huai Yong Zhu   M.Y. Zhu   12/08/2016

Name   Signature   Date

Article:

Photocatalytic Heck Cross-Coupling Reaction using Supported Palladium Nanoparticle as Catalysts

Fan Wang, Qi Xiao, Sarina Sarina and Huaiyong Zhu*

ABSTRAT

   Heck cross-coupling reactions have been catalyzed with supported palladium (Pd) photocatalysts, the nonplasmonic transition metal, under light irradiation in mild reaction condition with ligand free. This heterogeneous catalyst achieved high activity and selectivity in a wide range of Heck reactant substrates at atmospheric pressure and ambient temperature (50 °C) under light irradiation. After optimized conditions, we found that the catalyst with 1.0 wt% Pd loading supported on ZrO_2 achieved the best catalytic activity and selectivity. The photocatalytic performance was affected by several factors such as, solvent, base, reaction temperature. The reaction mechanism was proposed and the DFT calculations supported the proposed mechanism. Tuning the light intensity and wavelength of irradiation can manipulate the isomerization of cross-coupling product. Evidently, an effective and potential protocol is described and the results offer an alternative green route for more cross-coupling reaction and meanwhile, open a new door for more nonplasmonic metals contributing in more organic reactions not only as the thermal activated catalysts but also with their photocatalytic capabilities.

1. INTRODUCTION

   Cross-coupling reactions have been considered among the best direct routes in contemporary organic synthesis for the formation of C–C bonds.[1,2] In the view of cross-coupling reactions, Heck reaction was verified to be a significant method for C–C bond

formation in organic synthesis since it was first reported by Heck in 1968.[3] The C–C bond formation between aryl halide and olefins using both homogeneous and heterogeneous palladium (Pd) catalysts have been reported widely for the vinylation of aryl halides. In general, homogeneous Pd catalysts are used with phosphine ligands in the Heck reaction due to their high efficiency.[4,5] Despite their performance, the homogeneous Pd-based catalysis still suffers from various drawbacks such as high costs, non–reusability of catalyst as well as environmental pollutions caused by the heavy metal ions.[6] On the other hand, heterogeneous catalysis with phosphine–free Pd catalysts have attracted a great deal of attention as an easier and environmentally friendly alternative way to address the issue.[7,8] Significant progress have never terminated in the past few decades in developing Pd catalysts. However, all of these catalysts systems suffer from drawbacks included the high sensitivity of ligands towards air and moisture, complicated steps and high cost of the ligands. Also, usually these reactions are conducted at harsh conditions such as high temperature. The elevated temperature will produce unwanted side products and speed up the aggregation of Pd nanoparticles (NPs) dispersed on solid supports and thus damage the recyclability of the catalysts.[9] Therefore, highly efficiency and reusable catalyst systems with green chemical techniques and non-phosphine ligands are still recognized as an important objective for Heck reactions.

As per one of the principle of green chemistry stating that "the research should attempt to reduce the environmental impact of the chemical enterprise by developing a technology base that is inherently non–toxic to living things and the environment", it would be a meaningful breakthrough if we can achieve excellent catalytic activity of Pd catalysts under moderate condition meanwhile using one kind of low-cost, abundant and green energy source to minimize the environmental and economical impacts of chemical processes. Photocatalysis is particularly fascinating in the realm of green chemistry as it combines the efficiency of catalysis with the use of renewable resource – sunlight at moderate temperatures, which is an

immense achievement.[10-12] Nowadays, photocatalytic reactions under visible light have been applied extensively in organic synthesis.[13,14] We have extraordinary interest in using photocatalysis as an alternative way to drive organic synthesis transformations to achieve high activity and selectivity, such as visible light induced Suzuki-Miyaura cross coupling reactions using Pd NPs photocatalysts.[15] We believe that it is feasible to drive heck reaction by visible light, for its abundance, environmental impact and sustainability. Recently, we have demonstrated that light irradiation plays an essential role in cleaving carbon-halogen bond then facilitates the C–C bond formation through the activation of the reactants,[16] which is of great significance in Heck reaction. As nonplasmonic metal, Pd NPs strongly absorb the light mainly through interband electronic transitions, which is different from the way of plasmonic metals (gold, silver, and copper) – utilizing the localized surface plasmon resonance (LSPR) to enhance photocatalytic property.[17-20] We believed that light-excited electrons transfer form Pd NPs to the reactant molecules to induce and accelerate heck cross-coupling reaction. Under this context, we hypothesized that it was possible to design the Heck reaction with phosphine-free Pd photocatalysts induced by light with mild condition.

Herein we report on light irradiation with sodium acetate, a commercially available and efficient base as reaction medium with phosphine-free in Pd-catalyzed Heck reactions (C–C bond coupling) at mild conditions. We found that Pd/ZrO_2 photocatalyst exhibited excellent activity for Heck coupling under visible light irradiation at 50 °C and restrain the extends of formation of unwanted by-products, while no wanted product yield in the dark under identical conditions. In additional, our Pd NPs photocatalyst exhibited great tolerance for wide functional group on both reactants allows the convenient application at a direct route to assemble various important aryl halides and olefins. Based on the fundamental standard of green chemistry, it would be a highly breakthrough to design active, easily separable and

reusable catalyst systems that can catalyze such desired cross-coupling reaction under greener conditions.

2. EXPERIMENTAL SECTION

2.1 Chemicals

Zirconium (IV) oxide (ZrO_2, <100 nm particle size), palladium (II) chloride ($PdCl_2$, 99 %), sodium borohydride ($NaBH_4$, ≥98.0 %), and N,N-dimethylformamide (DMF, anhydrous, 99.8 %). The water used in all experiments was prepared by ultrapurification system.

2.2 Catalysts Preparation

PdNPs (1.0 wt% Pd supported on ZrO_2) were prepared by the impregnation-reduction method. To begin with, 2.0 g ZrO_2 powder was dispersed into 18.7 mL $PdCl_2$ (0.01 M) aqueous solution under continuous stirring at room temperature. Subsequently, added 5.3 mL lysine (0.1 M) aqueous solution while it was vigorously stirred for 30 min with kept the pH value in the range of 8−9. This suspension then was added dropwise 2 mL a freshly prepared aqueous $NaBH_4$ (0.35 M) solution. The mixture was aged for 24 h and after that, the solid was separated by centrifugation, washed with water three times and ethanol once. The washed solid was dried at 60 °C in a vacuum oven for 24 h. The dried powder was used directly as a catalyst. PdNPs (0.5-5.0 wt%) were prepared via a similar method by using different quantities of $PdCl_2$ aqueous solutions, lysine aqueous solution and aqueous $NaBH_4$ solution.

2.3 Activity Test

The photocatalytic reaction was conducted in a light reaction chamber. A 10 mL Pyrex glass tube (ϕ, 10 mm) was used as the reaction container. After adding the reactants and catalyst, the tube was filled in with Ar and sealed with a rubber septum cap. Then the tube was irradiated under a halogen lamp with the wavelength in the range of 400−750 nm

accompany stirring placed on a magnetic stirrer. The light intensity was altered to be 0.5 W/cm^2. In order to control the reaction temperature carefully, an air conditioner was set in front of the light-reaction chamber. The reaction temperature under irradiation was maintained the same as the reaction in the dark to make sure that the comparison is meaningful. The reactions in the dark were conducted using an oil bath placed on a magnetic stirrer. In order to strictly avoid exposure of the reaction to light, the tube was wrapped with aluminium foil. After the reaction, the reaction liquid was filtered through a Millipore filter (pore size 0.45 μm) to remove the solid photocatalyst particulates. The products were analyzed by an Agilent 6890 gas chromatography (GC) with HP−5 column. An Agilent HP5973 mass spectrometer was used to identify the product. For the different aryl iodide and olefins reaction, the products were analyzed and identified by gas chromatography mass spectrometer (GC-MS) including an Agilent HP5977A mass spectrometer attached to an Agilent 7890B gas chromatograph with a HP-5 column. Catalysts recycle experiment: after each reaction cycle, the solvent, substrate and products were removed by centrifugation; the separated catalyst was washed thoroughly with acetone twice, followed by centrifugal separation (5000 rpm, 10 min) and drying at 60 °C for 10 h. The resultant sample was used for recycle.

In the part of action spectrum, five light emission diode (LED) lamps were used as the irradiation source with the following wavelength: 400±5 nm, 460±5 nm, 520±5 nm, 590±5 nm, 620±5 nm. Except wavelength, all the other reaction conditions were controlled carefully to keep identical. The apparent quantum yield (AQY) was calculated as: AQY = [(Y_{light} − Y_{dark})/(the number of incident photons)] × 100, where Y_{light} and Y_{dark} are the amounts of products formed under light irradiation and dark conditions, respectively. The plot of AQE versus the respective wavelengths is the action spectrum of the reaction.

2.4 Catalysts Characterization

The transmission electron microscope (TEM) study and line profile analysis by an energy dispersion X-ray (EDX) spectrum technique of the photocatalysts were conducted on a JEOL 2100 TEM with an accelerating voltage of 200 kV. X-ray diffraction (XRD) patterns of the samples were collected by using a Philips PANalytical X'Pert PRO diffractometer with Cu Kα radiation (λ=1.5418 Å) at a fixed power source (40 kV and 40 mA). Scanning electron microscope (SEM) imaging, elemental mapping, and Energy Dispersive X-Ray Spectroscopy (EDS) were performed using a ZEISS Sigma SEM at accelerating voltages of 20 kV. Diffuse reflectance UV−visible (DR-UV−vis) spectra of the sample powders were examined with a Varian Cary 5000 spectrometer with $BaSO_4$ as a reference.

3. RESULTS AND DISSCUSSION

3.1 Supports

In the present study, Pd NPs supported on CeO_2, TiO_2, ZrO_2 and Al_2O_3 were prepared and the photocatalytic activity of theses supports was identified. We prepared this series of photocatalysts with 1.0 wt% Pd loading by the impregnation-reduction method.[21-24] Figure 1 shows the UV-visible (DR-UV-vis) spectra of Pd NPs on different supports. The light absorption of Pd NPs in the photocatalysts varies with the change of the supports, while the supports exhibit little absorption in the range of visible light (400-800 nm). According to the DR-UV-vis spectra, TiO_2 and CeO_2 can absorb most light with wavelength less than 400 nm and the Al_2O_3 shows the lowest absorption both in UV and visible light area. The ZrO_2 with Pd loading can absorb light around 400 nm, while the ZrO_2 support itself absorbs negligible light.

Table 1. Activity test of different supports for Heck reaction.[a]

27
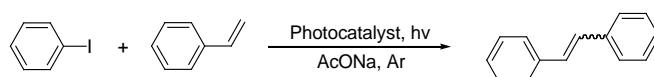
Entry	Catalyst	Incident light	Yield (%)[b]
1	Pd/ZrO$_2$ (1.0 wt%)	Visible	100
		Dark	0
2	Pd/Al$_2$O$_3$ (1.0 wt%)	Visible	82
		Dark	0
3	Pd/CeO$_2$ (1.0 wt%)	Visible	91
		Dark	0
4	Pd@TiO$_2$ (1.0 wt%)	Visible	100
		Dark	0
5	ZrO$_2$	Visible	0
		Dark	0

[a] Reaction conditions: photocatalyst 50 mg, iodobenzene 0.1 mmol, styrene 0.12 mmol, solvent DMF 2 mL, additive AcONa 50 mg, 1 atm Ar, environment temperature 50 ± 2 °C, reaction time 17 h. The visible light intensity was 0.5 W/cm^2. [b] The yields were calculated from the product formed and the reactant converted measured by GC.
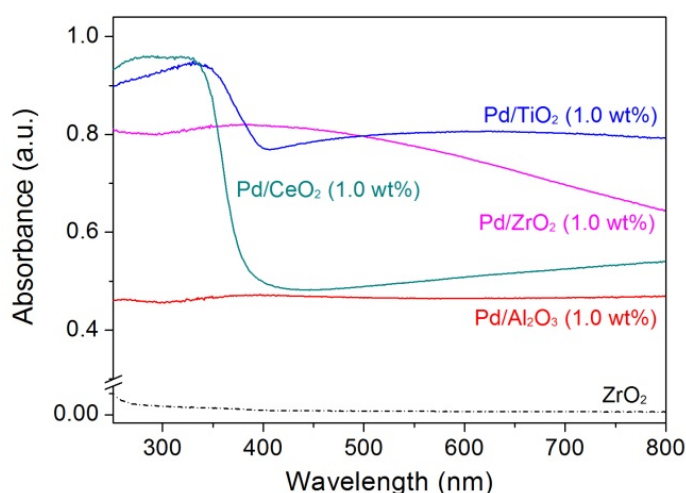
Figure 1. DR UV-vis spectra of the Pd NPs photocatalyst with various supports.

3.2 Pd loading

In our next stage, Pd NPs were supported on zirconia (ZrO$_2$) powder as photocatalysts (for the detailed method, see the Experimental Section) with various loading (0.5 wt%, 1.0 wt%, 1.5 wt%, 3.0 wt% and 5.0 wt%). The as-prepared catalysts were characterized with various techniques to confirm the composition and morphology. Figure 2 shows the transmission electron microscopy (TEM) analysis of the Pd NPs. The Pd NPs are distributed evenly on the

ZrO$_2$ particle surface and little agglomerations were observed with the increasing of Pd NPs loading on the support. The particles' diameter of the Pd NPs is concentrated mainly on 4 nm when the loading of Pd NPs are 0.5 and 1 wt% (Figure 2a and 2b). However the results will change to 5 nm when the loading is increased to 1.5, 3.0 and 5.0 wt%. (Figure 2c, 2d and 2e). Thus this method provides a simply process to prepare Pd NPs with average size around 5 nm, with Pd loading in the range from 0.5 to 5.0 wt%.
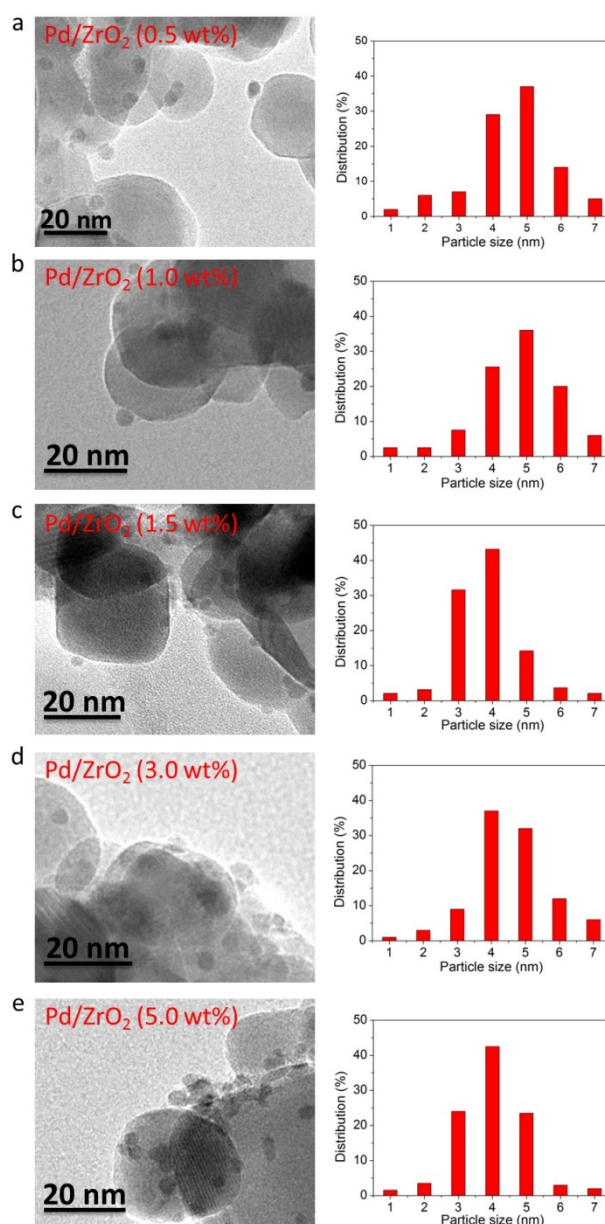
Figure 2. TEM images of the catalysts with different Pd loading and the relevant Pd particle size distribution. (a) Pd/ZrO$_2$ (0.5 wt%), (b) Pd/ZrO$_2$ (1.0 wt%), (c) Pd/ZrO$_2$ (1.5 wt%), (d)

Pd/ZrO$_2$ (3.0 wt%) and (e) Pd/ZrO$_2$ (5.0 wt%). The particle size distribution were calculated by measuring >200 isolate particles in the images of the corresponding catalyst.

Figure 3 shows the X-Ray diffraction (XRD) patterns of the catalysts with different Pd loading on ZrO$_2$. No reflection peaks Pd can be identified through XRD pattern of our photocatalysts, probably due to no loaded Pd large particles formed and Pd NPs were evenly dispersed on the support surface. This result suggests that the detection of metal NP signals in XRD patterns is closely related to the supporting materials (ZrO$_2$).
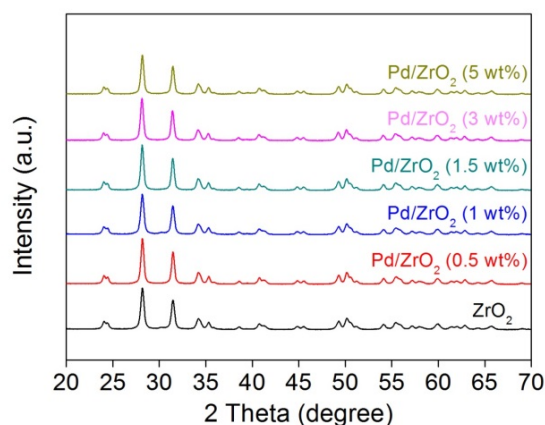
Figure 3. XRD patterns of catalysts with different Pd loading on ZrO$_2$.

The formation of various Pd NPs loading is also supported by the light absorption property and we investigated all the samples by diffuse reflectance DR-UV-vis spectra. As shown in Figure 4, ZrO$_2$ has a wide bang gap (5 eV),[23] and exhibits negligible light absorption above 400 nm, so the support contributes almost nothing to photocatalytic activity. On the other hand, Pd NPs catalyst with various loading on the ZrO$_2$ supports display high levels of absorption in the visible range, and the absorption increases with the increasing of Pd NPs loading. Thus the light absorption of the photocatalyst mainly origins from the Pd NPs loaded on the ZrO$_2$ support surface, and the interaction between the NPs and the ZrO$_2$ support could broaden the absorption peaks.
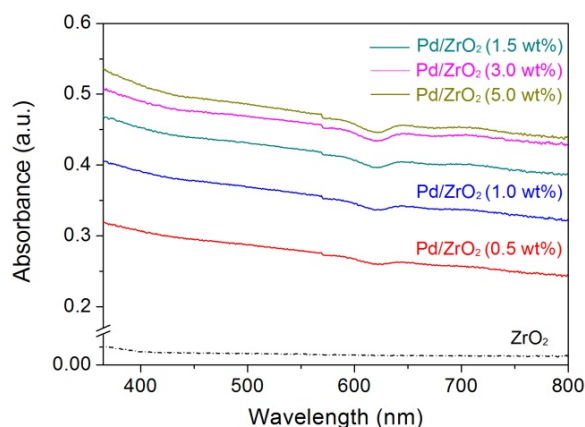
Figure 4. DR-UV-vis spectra of the Pd/ZrO$_2$ catalyst for various loading.

Photocatalysts with varying loading of Pd compositions show differences in the reaction conversions (Table2, entries 1-5). It was found that the photocatalytic efficiency of Pd NPs photocatalyst was significantly influenced by the metal content and the catalyst with 1.0 wt% Pd exhibited the best performance (Table 2, entry 2). The heck cross-coupling reaction was studied over the ZrO$_2$ support and Pd supported 0.5-5.0 wt%. With an increase in Pd loading the conversion of iodobenzene increases up to 1.0 wt% and above this loading the conversion slightly decreases. This is because of the increased NPs size and agglomeration of the nanoparticles into larger, less active clusters. An excellent yield (100%) of the desired cross-coupling product cis-stilbene and trans-stilbene were achieved under visible light irradiation within 17 h. Control experiments showed that no product yields in the dark while keep other experimental condition identical. This verifies that visible light irradiation completely facilitates the Heck cross-coupling reactions using the Pd/ZrO$_2$ (1.0 wt%) photocatalyst. To minimize the influence of heck reaction in the dark as well as considering of the high conversion under light irradiation, Pd/ZrO$_2$ (1.0 wt%) was selected to be the best appropriate photocatalyst for the further study.

Table 2. Heck reaction catalyzed using Pd/ZrO$_2$ photocatalysts with various Pd loading at 50 °C under visible light irradiation (red numbers) and in the dark (black numbers).[a]
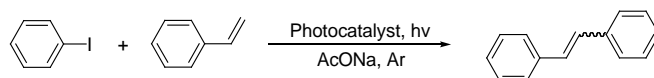
Entry	Catalyst	Incident light	Yield (%)[b]	TON[c]
1	Pd/ZrO$_2$ (0.5 wt%)	Visible	64	27
		Dark	0	0
2	Pd/ZrO$_2$ (1.0 wt%)	Visible	100	21
		Dark	0	0
3	Pd/ZrO$_2$ (1.5 wt%)	Visible	85	12
		Dark	24	3
4	Pd/ZrO$_2$ (3.0 wt%)	Visible	87	6
		Dark	24	2
5	Pd/ZrO$_2$ (5.0 wt%)	Visible	86	4
		Dark	35	1

[a] Reaction conditions: photocatalyst 50 mg, iodobenzene 0.1 mmol, styrene 0.12 mmol, solvent DMF 2 mL, additive AcONa 50 mg, 1 atm Ar, environment temperature 50 ± 2 °C, reaction time 17 h. The visible light intensity was 0.5 W/cm^2. [b] The yields were calculated from the product formed and the reactant converted measured by GC. [c] TON was calculated as $n_{product}/n_{Pd}$.

As the Pd/ZrO$_2$ (1.0 wt%) catalyst showing the optimal catalytic activity, we further investigate its detailed morphology by high resolution TEM (HR-TEM) and Scanning electron microscopy (SEM). Transmission electron microscopy (TEM) analysis of the Pd/ZrO$_2$ (1.0 wt%) (Figure 5a) shows Pd NPs uniformly dispersed on the surface of the ZrO$_2$ crystal. The mean diameter of the Pd NPs is less than 5 nm (Figure 5b). High resolution TEM (HR-TEM) in Figure 5c and 5d also confirmed the formation of the Pd NPs on the ZrO$_2$ crystal.
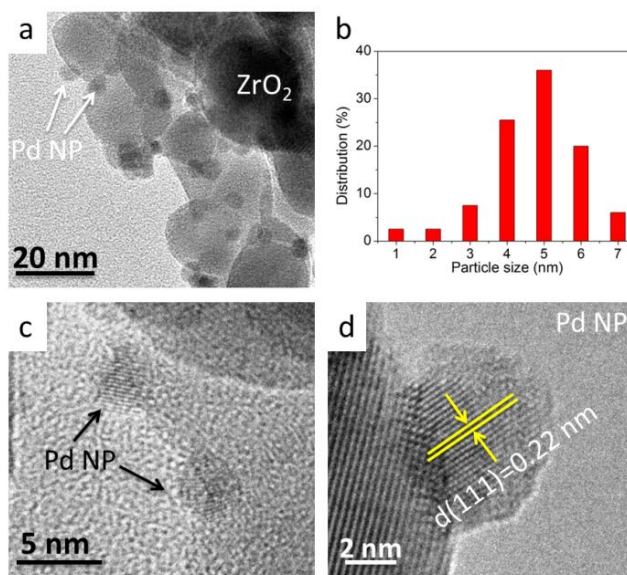
Figure 5. (a) TEM image of the Pd/ZrO$_2$ (1.0 wt%). (b) Particle size distribution of the Pd/ZrO$_2$ (1.0 wt%). (c and d) High-resolution TEM (HR-TEM) images of the Pd/ZrO$_2$ (1.0 wt%).

To investigate the elemental composition in the as-prepared photocatalyst, energy-dispersive X-ray spectroscopy (EDX) elemental mappings of the Pd/ZrO$_2$ (1.0 wt%) catalyst were performed (Figure 6a). EDX elemental mapping of the SEM image shows that all the components are homogeneously distributed throughout the sample. The percentages of Zr, O, and Pd elements in the catalysts were also analyzed from the EDX spectrum (Figure 6b), the Zr, O, and Pd are matched with the initial experimental design.
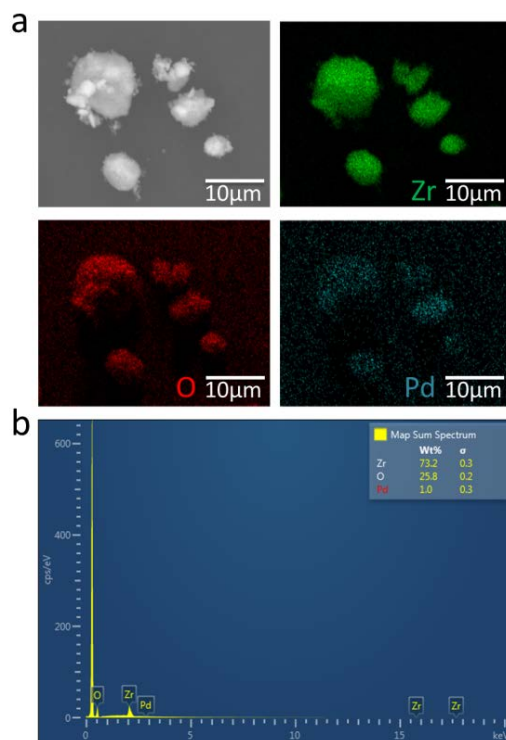
Figure 6. (a) Scanning electron microscopy (SEM) image of Pd/ZrO$_2$ (1.0 wt%) sample and the corresponding energy dispersive spectrometer (EDX) mapping of Zr, O, and Pd elements. (b) EDX spectrum.

3.3 Reaction condition

In a series of tests, heck cross-coupling reaction of Iodobenzene with styrene under various reaction conditions, such as solvents, bases, and reaction atmosphere, has been investigated using the Pd/ZrO$_2$ (1.0 wt%) catalyst under visible light irradiation (Table 3). Initially, we conduct the reaction under different atmospheres: argon, oxygen and air, respectively. It was found that inert gas atmosphere promoted the reaction greatly (Entries 1–3). There is no desired product be detected by GCMS under oxygen atmosphere. To verify the base effect in the Heck system, different bases were investigated in the cross coupling reaction. NaOAc was found to be the most effective base and was thus chosen as the preferred base for the reaction. The use of Na$_2$CO$_3$, KOH, NaOH and K$_2$CO$_3$ resulted in excellent yield of the desired product (Entries 4–7). This was attributed to the solubility of

bases in the solvent which directly affects the conversion of the reaction. Several commonly used solvents were tested in the reaction while other reaction conditions were maintained unchanged. The polar aprotic solvents, such as N, N-dimethylformamide (DMF), dimethyl sulfoxide (DMSO) afforded excellent yields of the coupling product (entries 1 and 10). The nonpolar solvents dichloromethane (CH_2Cl_2) and trifluorotoluene (BTF) gave a trace yield (Entries 11 and 12). The other relativity moderate polar solvents exhibited mediocre yields (Entries 13–15). This disciplinary results may due to the nonpolar solvents promoting a low amount of palladium leaching, gave low reaction rates for the heck reaction. That matches with the study Kohler et al. found for the Heck reaction of bromoacetophenone and styrene.[25] Generally, we found the following optimized conditions: using the Pd/ZrO_2 (1.0 wt%) photocatalyst, the reaction proceeded with 100% in DMF with NaOAc at 50 °C for 17 h under argon atmosphere (Entry 1).

Table 3. Influence of the reaction conditions for Heck cross-coupling reaction.[a]

Entry	Base	Solvent	Atmosphere	Yield (%)[b]
1	NaOAc	DMF	Ar	100
2	NaOAc	DMF	Air	65
3	NaOAc	DMF	O_2	Trace
4	Na_2CO_3	DMF	Ar	95
5	KOH	DMF	Ar	100
6	NaOH	DMF	Ar	86
7	K_2CO_3	DMF	Ar	91
8	NaOAc	DMSO	Ar	95
9	NaOAc	DMF	Ar	100
10	NaOAc	DMF	Air	65
11	NaOAc	BTF	Ar	Trace
12	NaOAc	CH_2Cl_2	Ar	Trace
13	NaOAc	DMA	Ar	36
14	NaOAc	Acetonitrile	Ar	9
15	NaOAc	IPA	Ar	4

[a] Reaction conditions: photocatalyst Pd/ZrO_2 (1.0 wt%) 50 mg, iodobenzene 0.1 mmol, styrene 0.12 mmol, solvent 2 mL, base 0.6 mmol, environment temperature 50 ± 2 °C, reaction time 17 h. The visible light intensity was 0.5 W/cm^2. [b] The yields were calculated from the product formed and the reactant converted measured by GC.

3.4 Light intensity and wavelength

We investigated the relationship between photocatalytic and the incident light (irradiance) and the results are depicted in Figure 7. When the irradiation intensity was increased from 0.1 to 0.2, 0.3, 0.4 and 0.5 W/cm^2 with keeping the other reaction conditions identical, the conversion of the reactions on the Pd NPs sequentially increased. The increased irradiance resulted in an almost linear increase in the conversion of heck cross-coupling reaction catalyzed by our Pd NPs. The conversion in the dark was regarded as the contribution of thermal effect. However, when the light intensity is 0 W/cm^2 (in the dark), there is no conversion in this reaction. Thus the thermal effect contributes nothing to promote the reaction. It can be seen in Figure, when the irradiance is 0.1 W/cm^2, the conversion for the reaction driven by light is only 15%, and when the irradiance rose to 0.5 W/cm^2, 100% product yield was achieved due to light irradiation. The increased irradiance results in more photon in unit interval, thus excites more electrons to form light-excited energetic electrons, which give a higher reaction rate. Moreover, we also found that the light intensity can affect the stereoselectivity of the reaction. The highest selectivity of cis-stilbene was obtained when the light intensity reached highest (0.5 W/cm^2), and the selectivity increased with the increasing of light intensity. In other words, the formation of cis-stilbene in a major amount compared to trans-stilbene with the increased light intensity. Such photochemical isomerization of stilbene could probably be affected when exposed to the light. The mechanism for the trans to cis isomerization is still indeterminate,[26] however, we verified that higher the light intensity could facilitate this process. This result gives us an operable way to manipulate the selectivity of stilbene isomeride by changing the intensity of light.
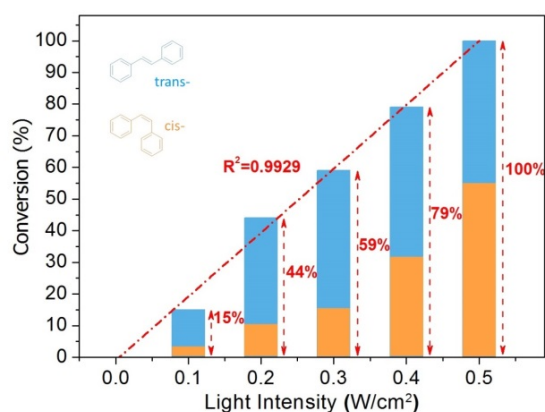
Figure 7. Dependence of the catalytic activity of Pd NPs for Heck cross-coupling reaction. The red number with percentages shows the contribution of the light irradiation effect.

To further understand the effect of light irradiation and explore the photocatalytic mechanism, the dependence of photocatalytic rate on wavelength of light was investigated. A useful tool to clarify the relationship between them is the action spectrum (the rate of reaction activity plotted against wavelength of light).[27,28] It could show the mapping between the wavelength-dependent photocatalytic rate and the light absorption spectrum. We conducted heck cross-coupling reaction using Pd/ZrO$_2$ (1.0 wt%) catalyst at 50 °C under irradiation with different wavelength. Five LED lamps with wavelength 400 ± 5 nm, 460 ± 5 nm, 520 ± 5 nm, 590 ± 5 nm, 620 ± 5 nm were used as the irradiation source, respectively. The photocatalytic rates were calculated to the apparent quantum yield (AQY). As shown in Figure 8, the red plots, represent the AQY value, versus the corresponding wavelength are the action spectrum. The trend of AQY well tracks the light absorption curve of Pd/ZrO$_2$ (1.0 wt%) photocatalyst. This result demonstrated that heck reaction is mainly through a photo-induced process not a thermo-catalytic process, as the change of wavelength in the irradiation has significant impact on the conversion rate. In the present action spectrum, the highest yield was obtained when the reaction system exposed under irradiation with the shortest wavelength (400 nm). The product yield decreased regularly following the trend of absorption spectrum of Pd/ZrO$_2$ (1.0

wt%) photocatalyst with the wavelength increased. The photons of shorter wavelength are capable of excite metal electrons to higher energy level, which can enhance the possibility of transfer these energetic electrons to the reactant molecules absorbed on Pd NPs surface to induce reaction. Therefore when the light intensity kept identical, the shorted the wavelength, the greater the AQY.
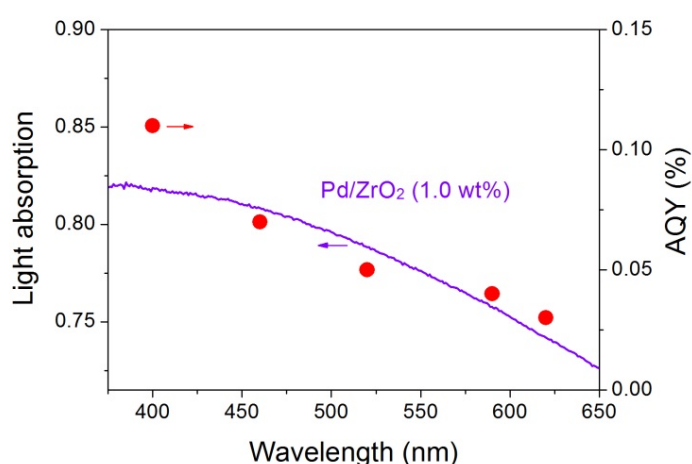
Figure 8. Photocatalytic action spectrum for heck cross-coupling reactions. The light absorption spectra (left axis) is DR-UV-vis spectra of Pd/ZrO$_2$ (1.0 wt%). The AQY values were calculated on the basis of this experiment.

In additional, the light wavelength can also remarkably affect the stereoselectivity of the product and the results are listed in Table 4. When the cross-coupling of Iodobenzene and styrene are conducted under light irradiation with wavelength >400 nm, 100% yield of trans-stilbene were obtained and there is no cis-stilbene observed. While, when light wavelength changed to 400 nm, 50% of each stilbene isomers were found in the product. The possible reason for that phenomenon is that the energy required in each step is different. We speculate that the reaction sequence of our cross-coupling reaction is first yield trans-stilbene and the trans-stilbene subsequently transform to cis-stilbene through photochemical isomerization. This process was commonly considered occurs in the excited state through rotation around the C=C double bond. As transfer energetic electrons to the second step product (cis-stilbene)

require greater energy than that to first step product (trans-stilbene), light with short wavelength (400 nm) can excite metal electrons to higher energy level thus had great possibility to convert trans isomer to cis isomer.

Table 4. Performance of Pd/ZrO$_2$ (1.0 wt%) photocatalyst in Heck reaction with irradiation of different wavelength.[a]

Wavelength (nm)	AQY (%)	Conv. (%)	Select. (%)	
			Cis-stilbene	trans-stilbene
400	0.11	68	50	50
460	0.07	54	0	100
520	0.05	40	0	100
590	0.03	35	0	100
620	0.04	32	0	100

[a] Reaction conditions: photocatalyst 50 mg, iodobenzene 0.1 mmol, styrene 0.12 mmol, solvent DMF 2 mL, 1 atm Ar, additive AcONa 50 mg, environment temperature 50 ± 2 °C, reaction time 17 h. The visible light intensity was 0.2 W/cm^2. The conversion were calculated from the product formed and the reactant converted measured by GC.

3.5 Reaction temperature

Temperature is another important feature for our Pd NP photocatalytic system as the catalytic activity can be increased by elevating the reaction temperature.[19,20] For example, the conversion of our heck system at 35 °C was only 30%, while the extent of conversion achieved 100% when the temperature was elevated to 50 °C (Figure 9, red pentagons). Also, higher conversion was achieved in the dark when raising the reaction temperature. For example, only 6% conversion was obtained when the temperature is 60 °C, whereas the 100% conversion was reached when raising the temperature to 100 °C (Figure 9, gray circles). When the reaction temperature did not exceed 50 °C, the photoexcitation contributes completely to the catalytic activity and the thermal effect has no contribution. This result verified that such reactions involving the interaction between light-excited electrons and reactant molecules, the prerequisite to drive them is not the high reaction temperature but the

light irradiation. Because light irradiation can drive the reaction at low reaction temperature only with the yield of excited electrons possess sufficient energy. When the reaction temperature was raised to 60 °C, the catalytic activity began to appear in the dark reaction and increased sharply attained to 100% at 100 °C. At a higher temperature, thermal activated electrons of the metal NPs populate higher energy level, even without light irradiation, it still possess greater chance to surmount the activation barrier thus induce the reaction. In contrast, at lower reaction temperature, the thermal effect is insufficient to activate electrons of metal NPs to overcome the activation barrier without the assistance of irradiation.
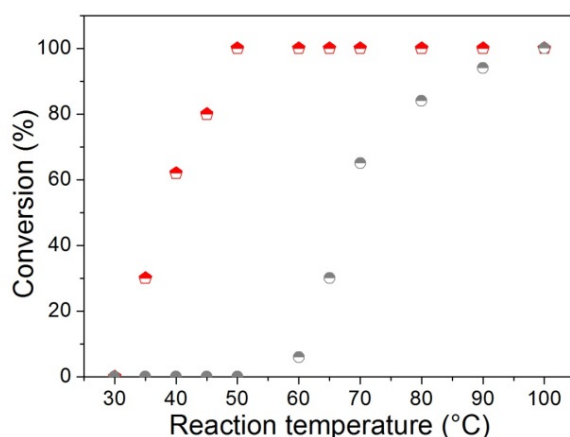
Figure 9. Dependence on catalytic activity on different reaction temperatures for Heck cross-coupling reaction under a thermal process in the dark (gray circles) and the light irradiation process (red pentagons). Iodobenzene and styrene were used as cross-coupling reactants under light irradiation and in the dark.

In additional, we also calculated the apparent activation energies with different photocatalytic yield of the Pd NP photocatalyst at varies temperatures in both light and dark by using the Arrhenius equation. The kinetic data for photocatalytic reactions was choose in the range of 30-50 °C, and the range of 60-100 °C was selected for the thermal reaction. As showm in Figure 10, the calculated activation energy is 128.7 kJ/mol for the Heck reaction in the dark,

while it is 80.1 kJ/mol for the photocatalytic reaction under irradiance. Thus, light irradiation can reduce the activation energy of the Heck reaction by 48.6 kJ/mol, which means 38% activation energy is the "uncatalyzed" part.
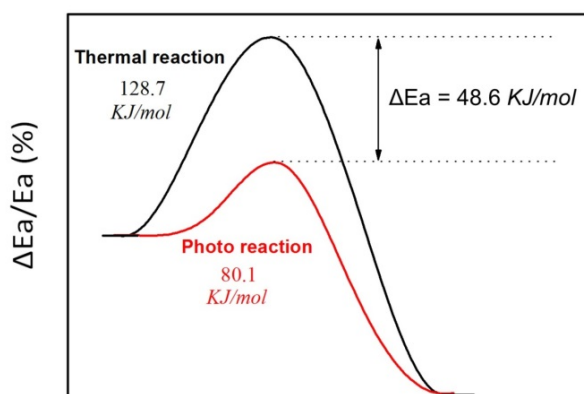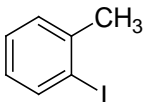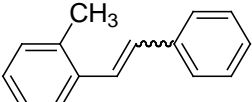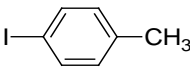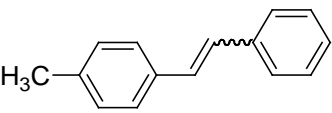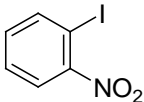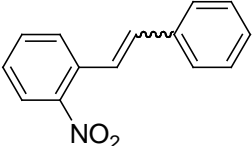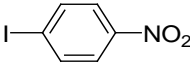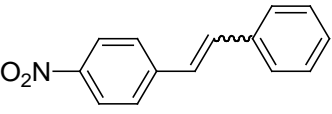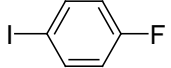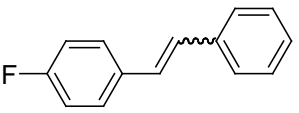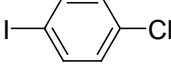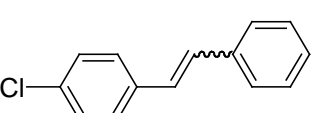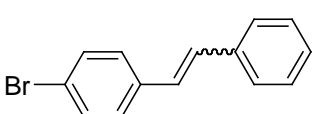
Figure 10. Apparent activation energy reduction of the Heck reaction caused by the light irradiation and on the Pd NP photocatalyst.
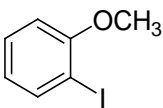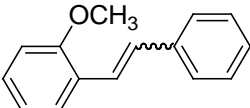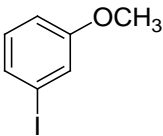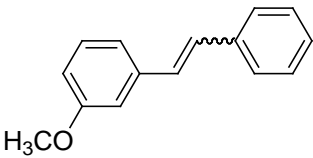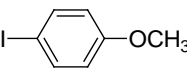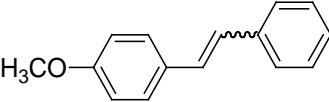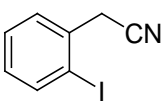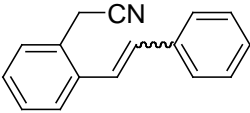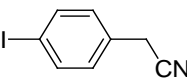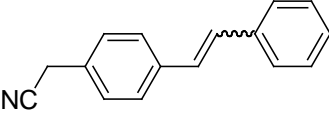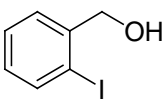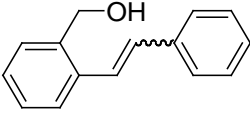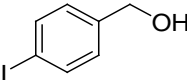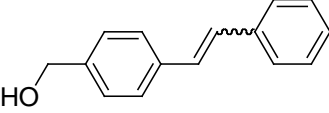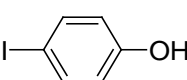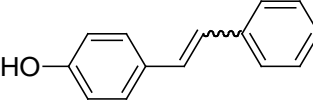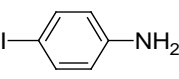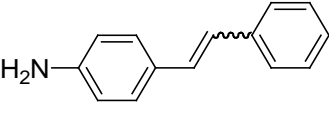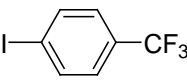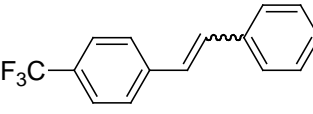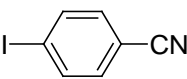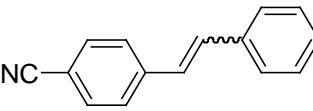
3.5 Functional group
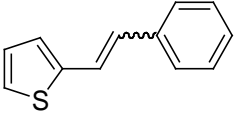
With the obtained optimized conditions, various substituted aryl iodides and olefins were tested and the results were summarized in Table 5. Generally, the reaction yield the desired products in good to excellent yields (68-100%) for aryl iodides and styrene under light irradiation and in discrepant low yields in the dark (under 25%) with other condition identical. It was found that the catalyst works well with both electron withdrawing and electron don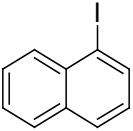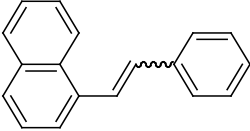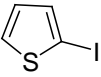ating substituents. However, among the various cross-coupling reactions of styrene and aryl iodides possessing electron-withdrawing and electron-donating group, the electron-donating group showed a slight decrease in reactivity compared with the electron-withdrawing group. Aryl iodides with electron-withdrawing group on para position will influence reaction activity according to their capacity of electron withdrawing. It should be noted that when aryl halides with the weak electron-withdrawing group (Entries 5 and 6) reacted with styrene, content yields (85% and 71%) were achieved. However, when the same

situation comes to 1-Iodo-4-nitrobenzene and 4-Iodobenzonitrile (Entries 4 and 18), the strong electron-withdrawing groups gave lower yield (64% and 51%) even increased reaction temperature. On the other hand, aryl iodides with electron donating groups required prolonged reaction time to achieve excellent yields (Entry 16). Furthermore, the aryl iodides with substituted groups in ortho and meta positions afforded lower yields compared with para-isomers (Entries 3 and 4, 13 and 14), which may due to the steric hindrance. In additional, the coupling of styrene with 2-iodothiophene (Entry 20) gave the corresponding products in 73% yields at enhanced temperature (60 °C).

Table 5. Pd/ZrO$_2$ (1.0 wt%) catalyzed Heck reaction of styrene with various iodobenzene substrates.[a]

Entry	Substrates	t (h)	Product	Conv. (%)[b]	Select. (%)	Yield (%)
1		17		64 (0)	96 (0)	61 (0)
2		17		87 (6)	100 (100)	87 (6)
3[d]		24		100 (0)	19 (0)	19 (0)
4[d]		24		100 (0)	64 (0)	64 (0)
5		17		85 (12)	100 (85)	85 (10)
6		17		73 (10)	97 (83)	71 (8)
7		17		60 (10)	100 (95)	60 (10)
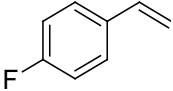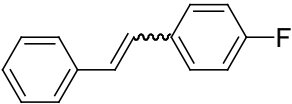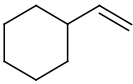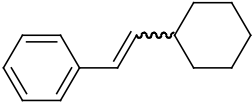
	Substrate	Time	Product			
8	OCH₃ / I (2-iodoanisole)	17	(E)-2-methoxystilbene	80 (3)	77 (100)	62 (3)
9	OCH₃ / I (3-iodoanisole)	17	(E)-3-methoxystilbene	100 (11)	100 (100)	100 (11)
10	I—OCH₃ (4-iodoanisole)	17	4-methoxystilbene	80 (0)	100 (0)	80 (0)
11	CN / I	24		100 (0)	100 (0)	100 (0)
12	I—CN	17		76 (0)	66 (0)	50 (0)
13	OH / I	17		42 (0)	100 (0)	42 (0)
14	I—OH	17		100 (0)	49 (0)	49 (0)
15	I—OH	17		68 (0)	100 (0)	68 (0)
16[d]	I—NH₂	24		100 (33)	100 (50)	100 (17)
17	I—CF₃	17		88 (6)	90 (67)	79 (4)
18[c]	I—CN	24		62 (24)	82 (100)	51 (24)
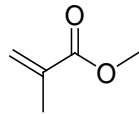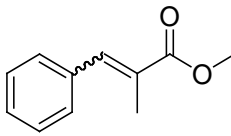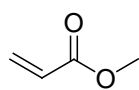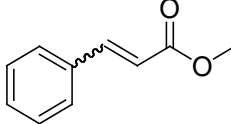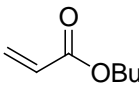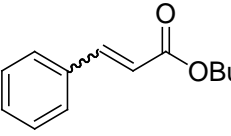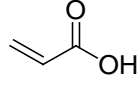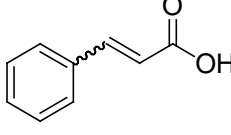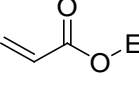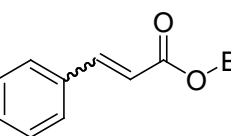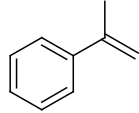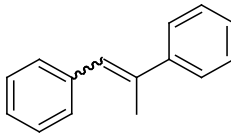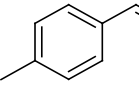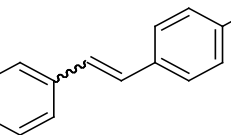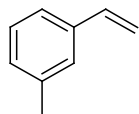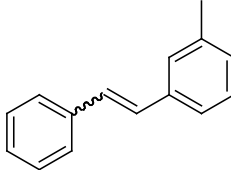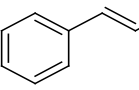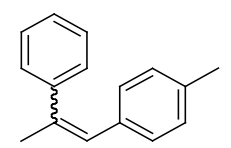
19		17		93 (90)	100 (2)	93 (18)
20[c]		17		73 (0)	100 (0)	73 (0)

[a] Reaction conditions: photocatalyst 50 mg, iodobenzene substrates 0.1 mmol, styrene 0.12 mmol, solvent DMF 2 mL, additive AcONa 50 mg, 1 atm Ar, environment temperature 50 ± 2 °C. The visible light intensity was 0.5 W/cm^2. The values in the parentheses are the results in the dark. [b] The conversion were calculated from the product formed and the reactant converted measured by GCMS. [c] 60 °C. [d] 80 °C.

Various olefins with iodobenzene for heck reaction were subsequently investigated and the results are summarized in Table 6. The present catalyst system effectively converted Butyl acrylate in excellent yield (Entry 4). Excellent catalytic activity were observed in the couplings of 4-Fluorostyrene (Entry 1). Also, it was found that the reaction also proceeded nicely with the aliphatic olefin Vinylcyclohexane (Entry 2). Obviously, electron-deficient terminal olefins provided the desired products in lower yields than electron-rich terminal olefins did (Entries 4 and 5). Furthermore, the terminal olefins with substituted groups in para positions gave higher yields in comparison with meta position (Entries 9 and 10).

Table 6. Pd/ZrO$_2$ (1.0 wt%) catalyzed heck reaction of iodobenzene with various olefins.[a]

Entry	Substrates	t (h)	Product	Conv. (%)[b]	Select. (%)	Yield (%)
1		17		94 (0)	100 (0)	94 (0)
2		17		81 (0)	100 (0)	81 (0)

Entry	Substrate	Time	Product			
3	methyl methacrylate	24	methyl α-methylcinnamate	86 (21)	52 (84)	45 (18)
4[d]	methyl acrylate	17	methyl cinnamate	84 (6)	100 (100)	84 (6)
5[d]	butyl acrylate (OBu)	17	butyl cinnamate (OBu)	96 (35)	88 (28)	85 (10)
6[c]	acrylic acid (OH)	24	cinnamic acid (OH)	100 (0)	96 (0)	96 (0)
7[d]	ethyl acrylate (O–Et)	17	ethyl cinnamate (O–Et)	88 (18)	100 (100)	88 (18)
8[c]	α-methylstyrene	24	1,1-diphenylpropene	100 (36)	70 (87)	70 (31)
9	4-methylstyrene	17	(4-methyl) stilbene	100 (0)	100 (0)	100 (0)
10	3-methylstyrene	17	(3-methyl) stilbene	72 (14)	98 (99)	71 (14)
11[c]	(E)-β-methylstyrene	24	methyl(4-methylphenyl) styrene	100 (21)	83 (88)	83 (18)

45

3.6 Proposed mechanism

Scheme1. Schematic mechanisms of the Heck reaction pathways with supported Pd NPs under light irradiation.

Combined our experimental results and the previous literature reports,[29-34] a plausible reaction pathway was proposed (Scheme 1). The presented Heck cross-coupling reaction involves two essential steps: (1) breaking the C-I bond in aryl iodide, and (2) activation of the styrene molecules which then facilitate insertion.[35,36] It has been widely studied that electron transfer from the Pd atoms to the halogen atoms is regarded as the rate-determining step and involved in facilitating the carbon−halogen bond cleavage in the Pd heterocatalysis.[1,9,37] In the present study, upon sunlight irradiation, enhanced catalytic activity was observed. The Pd

NPs strongly absorb the light mainly through interband electronic transitions which excites the electrons of the Pd NPs to the high-energy band. It is believed that the light-excited electrons at the surface of the Pd NPs can enhance the catalytic ability as the reaction occurs on the surface of Pd NPs. According to our previous study of DFT calculations, when one electron enters an unoccupied orbital, the C-I bond elongates from 0.214 to 0.300 nm, thus making it easier to be cleaved.[16] According to the simulation study, we can see that irradiation plays an essential role in the catalytic mechanism of Heck reaction through the activation of the reactants. There is one most interesting feature should be noticed is that the selectivity of isomeric products. According to our investigation, the yield of cis stilbene (Z-stilbene) and trans-stilbene (E-stilbene) is involved in light intensity and wavelength. Depending upon our investigation, one can have irradiance-dependent and wavelength-dependent selection of the desired isomeric product.

3.7 Recycle

For the property of heterogeneous catalyst, the reusability is a very practical factor, particularly when precious metals are used. To clarify this issue, the performance of our catalytic systems was tested for the iodobenzene and styrene model chemical transformation up to five consecutive cycles and the results are illustrated in Figure 11. The reaction conditions were kept unchanged for each run and after each reaction cycle, and the catalyst was separated by centrifugation. After each cycle, the catalyst was washed with acetone twice and then dried for subsequent reactions. As portrayed in Figure 11, experimental results indicate that the catalyst is able to reuse without losing significant activity and selectivity (cis-stilbene and trans-stilbene) can be maintained >99%. In additional, each of the isomer kept stable selectivity for each run. The observed slightly drop in catalytic activity was possibly because of the loss of Pd NPs during washing after each run.
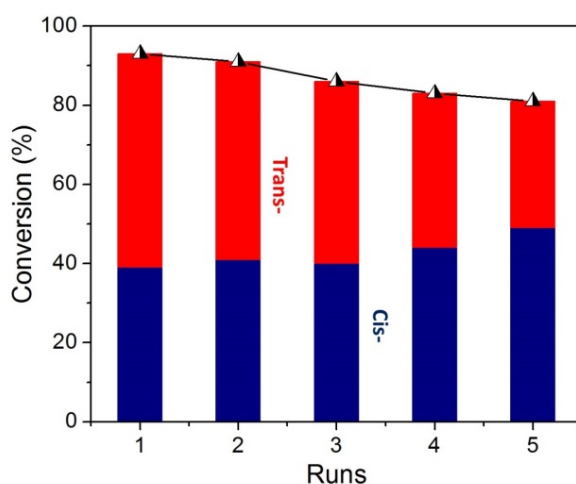
Figure 11. The recyclability of the Pd/ZrO$_2$ (1.0 wt%) for the Heck reaction using iodobenzene and styrene as the substrates under visible light irradiation. Reaction conditions: iodobenzene (0.1 mmol), styrene (0.1 mmol), Pd/ZrO$_2$ (1.0 wt%) photocatalysts (50 mg), NaOAc (50 mg), 2 mL DMF, environmental temperature 50 °C, reaction time 17 h, light intensity 0.5 W/cm^2.

4. Conclusions

To sum up, we depicted a protocol for highly effective and selective driving Heck cross-coupling reaction by using Pd NPs photocatalyst, which performed under light irradiation through a "green process" without intensive heating and pressure, ligand and strong base. The conversion of the reaction can be optimized by rising light intensity and reaction temperature. Furthermore, the present catalytic system can be applied in catalyze a variety of aryl iodide and styrene substrates effectively. The selectivity of E and Z isomeric product can be affected by tuning the light intensity and wavelength of irradiation. Meanwhile, Our Pd NPs catalyst is efficiently reusable for several times without significantly losing activity, which showing its great heterogeneous advantage. The finding of this study may inspire further exploration on novel efficient catalytic systems for a wide range of cross-coupling using supported PdNP catalysts.

Acknowledgements

Reference list:

1. A. Meijere and F. Diederich, *Metal-Catalyzed Cross-Coupling Reactions,* Wiley-VCH, Weinheim, 2004, vol. 1–2.

2. A. F. Littke and G. C. Fu, *Angew. Chem. Int. Ed.,* 2002, **41***,* 4176-4211.

3. R. F. Heck, *J. Am. Chem. Soc.,* 1968, **90,** 5518-5526.

4. F. Y. Zhao, B. M. Bhanage, M. Shirai and M. Arai, *J. Mol. Catal. A: Chem.,* 1999, **142,** 383-388.

5. I. P. Beletskaya and A. V. Cheprakov, *Chem. Rev.,* 2000, **100,** 3009-3066.

6. H. J. Li and L. Wang, *Eur. J. Org. Chem.,* 2006, **22,** 5099-5102.

7. A. F. Schmidt and V. V. Smirnov, *J. Mol. Catal. A: Chem.,* 2003, **203,** 75-78.

8. C. Gurtler and S. L. Buchwald, *Chem. Eur. J.,* 1999, **5,** 3107-3112.

9. Á. Molnár, *Chem. Rev.,* 2011, **111,** 2251-2320.

10. G. Palmisano, V. Augugliaro, M. Palmisano and L. Palmisano, *Chem. Commun.,* 2007, 3425-3437.

11. M. Fagnoni, D. Dondi, D. Ravelli and A. Albini, *Chem. Rev.,* 2007, **107,** 2725-2756.

12. S. Navalon, R. Martin, M. Alvaro and H. Garcia, *ChemSusChem,* 2011, **4,** 650-657.

13. D. A. Nicewicz and D. W. C. MacMillan, *Science,* 2008, **322,** 77-80.

14. D. A. Nagib, M. E. Scott and D. W. C. MacMillan, *J. Am. Chem. Soc.,* 2009, **131,** 10875-10877.

15. Q. Xiao, S. Sarina, E. Jaatinen, J. F. Jia, D. P. Arnold, H. W. Liu and H. Y. Zhu, *Green Chem.,* 2014, **16,** 4272-4285.

16. S. Sarina, H. Y. Zhu, Q. Xiao, E. Jaatinen, J. F. Jia, Y. M. Huang, Z. F. Zheng and H. S. Wu, *Angew. Chem. Int. Ed.,* 2014, **53,** 2935-2940.

17. X. Chen, H. Y. Zhu, J. C. Zhao, Z. F. Zheng and X. P. Gao, *Angew. Chem. Int. Ed.,* 2008, **120,** 5433-5436.

18. H. Y. Zhu, X. B. Ke, X. Z. Yang, S. Sarina and H. W. Liu, *Angew. Chem. Int. Ed.,* 2010, **122,** 9851-9855.

19. S. Linic, P. Christopher and D. B. Ingram, *Nat. Mater.,* 2011, **10,** 911-921.

20. P. Christopher, H. L. Xin, A. Marimuthu and S. Linic, *Nat. Mater.,* 2012, **11,** 1044-1050.

21. S. Sarina, H. Y. Zhu, E. Jaatinen, Q. Xiao, H. W. Liu, J. F. Jia, C. Chen and J. Zhao, *J. Am. Chem. Soc.,* 2013, **135,** 5793-5801.

22. Y. L. Zhang, Q. Xiao, Y. S. Bao, Y. J. Zhang, S. Bottle, S. Sarina, B. Zhaorigetu and H. Y. Zhu, *J. Phys. Chem. C,* 2014, **118**, 19062-19069.

23. X. Chen, H. Y. Zhu, J. C. Zhao, Z. F. Zheng and X. P. Gao, *Angew. Chem., Int. Ed.,* 2008, **47**, 5353-5356.

24. H. Y. Zhu, X. Chen, Z. F. Zheng, X. B. Ke, E. Jaatinen, J. C. Zhao, C. Guo, T. F. Xie and D. J. Wang, *Chem. Commun.,* 2009, 7524-7526.

25. K. Köhler, R. G. Heidenreich, J. G. E. Krauter and J. Pietsch, *Chem. Eur. J.,* 2002, **8,** 622-631.

26. D. H. Waldeck, *Chem. Rev.,* 1991, **91,** 415-436.

27. E. Kowalska, R. Abea and B. Ohtania, *Chem. Commun.,* 2009, **2,** 241-243.

28. A. Tanaka, S. Sakaguchi, K. Hashimoto and H. Kominami, *ACS Catal.,* 2013, **3,** 79-85.

29. G. Xie, P. Chellan, J. Mao, K. Chibale and G. S. Smith, *Adv. Synth. Catal.,* 2010, **352,** 1641-1647.

30. H. Hagiwara, Y. Sugawara, T. Hoshi and T. Suzuki, *Chem. Commun.,* 2005, **23,** 2942-2944.

31. H.-J. Xu, Y.-Q. Zhao and X.-F. Zhou, *J. Org. Chem.,* 2011, **76,** 8036-8041.

32. X. Zhou, J. Luo, J. Liu, S. Peng and G.-J. Deng, *Org. Lett.,* 2011, **13,** 1432-1435.

33. B. Schmidt and N. Elizarov, *Chem. Commun.,* 2012, **48,** 4350-4352.

34. A. Modak, J. Mondal, M. Sasidharan and A. Bhaumik, *Green Chem.,* 2011, **13,** 1317-1331.

35. L. Q. Xue and Z. Y Lin, *Chem. Soc. Rev.,* 2010, **39,** 1692-1705.

36. F. Diederich and P. Stang, *Metal-catalyzed Cross-coupling Reactions,* Wiley-VCH: Weinheim, Germany, 1998.

37. M. Turner, V. Golovko, O. Vaughan, P. Abdulkin, A. Murcia, M. Tiskhov, B. Johnson and R. Lambert, *Nature,* 2008, **454,** 981-983.

Chapter 3:

Supported Gold Nanoparticles for Organic Synthesis under mild condition

Introductory Remarks

In this chapter, we designed the Au NPs supported on ZrO_2 as catalyst to synthesize long aliphatic esters by the one-step catalytic self-esterification of primary alcohols under mild condition. As esters are traditional produced via a multistep process which results in a significant amount of by-product, our protocol stands out in comparison with the traditional way.

We prepared Au NPs supported on ZrO_2 with different loading and investigated the relationship between the catalysts performance and their corresponding particle size and distribution. Various solvents and bases were also selected in our reaction system and the resulted optimal condition showed the excellent conversion and selectivity of esters. This thermal Au catalyzed process exhibited well tolerance for a wide range of less reactive straight-chainalcohols (C_4-C_{12}) at ambient temperature and also as a heterogeneous catalyst, it is available to reuse without significant activity loss. Our study inspires further studies to simplify multiple-step reaction pathway by another metal as catalyst. Furthermore, we plan to find more application of this Au NPs photocatalyst.

Statement of Contribution of Co-Authors

Publication title and date of publication or status:

Highly efficient self-esterification of aliphatic alcohols using supported gold nanoparticles under mild conditions

Fan Wang, Qi Xiao*, Pengfei Han, Sarina Sarina and Huaiyong Zhu

Published on *Journal of Molecular Catalysis A: Chemical*

Article first published online: 11 Jun. 2016, DOI:10.1016/j.molcata.2016.06.010.

Contributor	Statement of contribution
Student Author: Fan Wang Signature: *Fan* Date: 12/08/2016	Discovered the photocatalytic reaction, organized and designed the experiments, conducted the data collection, analyzed the data, proposed the reaction mechanism and wrote the manuscript
Pengfei Han	Analyzed data, provided the detailed BET analysis
Sarina Sarina	Revised paper and discussed on the reaction
Qi Xiao	Give constructive suggestion on the reaction and polished the manuscript
Prof. Huaiyong Zhu	Proposed the idea

Principal Supervisor Confirmation

I have sighted email or other correspondence from all Co-author confirming their certifying authorship.

<table>
<tr><td>Huai Yong Zhu</td><td>H. Y. Zhu</td><td>12/08/2016</td></tr>
<tr><td>Name</td><td>Signature</td><td>Date</td></tr>
</table>

Article:

Highly efficient self-esterification of aliphatic alcohols using supported gold nanoparticles under mild conditions

Fan Wang, Qi Xiao,* Pengfei Han, Sarina Sarina and Huaiyong Zhu

Abstract

Long aliphatic esters were prepared by the one-step catalytic self-esterification of primary alcohols using molecular oxygen as a green oxidant and supported gold nanoparticles (Au NPs) as catalyst. This heterogeneous catalyst achieved high activity and selectivity in a wide range of less reactive straight-chain alcohols (C_4-C_{12}) at atmospheric pressure O_2 and near ambient temperature (45 °C). Under optimised conditions, the catalyst with Au loading of 3 wt% achieved the highest catalytic activity and selectivity. The AuNP catalysts are efficient and readily recyclable. The finding of this study may inspire further studies on new efficient catalytic systems for a wide range of organic syntheses using supported AuNP catalysts.

1. Introduction

The synthesis of esters is one of the fundamental and important transformations in organic synthesis [1-7]. Esters are conventionally produced, both in industry and in laboratories, through condensation of carboxylic acid or activated acid derivatives with alcohols via a multistep process, in an acid catalytic system or the presence of a dehydrating agent [8-11]. That results in large amounts of unwanted by-products and a significant amount of waste. Therefore, a more economic and sustainable way to synthesize esters is still considered as an important objective in the field organic chemistry [12-14]. In this respect, developing catalytic process that can directly convert alcohols [15], the easily accessed bulk chemicals [16], into corresponding esters constitutes a key tool towards sustainable production and the improvement in the field of catalysis. Among the studies on the catalytic reaction on alcohols,

the direct transformation of aliphatic alcohols to corresponding esters has received less attention than that of more reactive benzylic alcohols, as aliphatic alcohols are chemically stable and it is rather challenging to conduct the transformation under mild reaction conditions. To the best of our knowledge, only few examples were reported on the direct self-esterification of aliphatic alcohols [17-23], while most of these processes result in the corresponding aldehydes and acids as the by-products. Previously reported works, mainly homogeneous catalytic systems [17,24-27], required harsh reaction conditions such as high temperatures and pressure. In addition, most of these processes have several drawbacks on both environmental and operational aspects, such as employment of toxic metal complexes as catalysts, long reaction time or reusability of catalysts.

Therefore, the development of efficient heterogeneous catalyst for the self-esterification of aliphatic alcohols to corresponding esters continues to attract significant interest (see Table 1). For example, Ishida and co-workers reported that Au/CeO_2 produces octyl octanoate directly from 1-octanol with a 54% yield [28]. Beller et al. reported direct oxidative esterification of aliphatic alcohols over easily reusable Co_3O_4-N@C catalysts [29]. The Co catalysts showed excellent activity, whereas the reaction needs to be conducted under 1 bar of O_2 and 120 °C. Apart from oxidative esterification, an acceptorless dehydrogenative coupling of aliphatic alcohols to esters by heterogeneous Pt catalysts (Pt/SnO_2) was also reported in N_2 under solvent-free conditions [30]. Overall these processes still require high temperatures and pressures, thus developing an efficient heterogeneous catalytic system for the self-esterification of aliphatic alcohols under mild conditions has great significance in both economic and industry aspect.

Table 1. Comparison of the reaction conditions and catalytic activity of various heterogeneous catalysts reported in the literatures for the direct esterification of 1-octanol to octyl octanoate.[a]

Entry	Catalysts	Conditions[a]	Yield (%)
1	Au/CeO$_2$ [ref.28]	80 °C, 0.5 MPa O$_2$, 6 h	54
2	Co$_3$O$_4$-N@C [ref.29]	120 °C, 1 bar O$_2$, 24 h, K$_3$PO$_4$	75
3	Pt/SnO$_2$ [ref.30]	180 °C, 1 atm N$_2$, 36 h	98
4	Au/HT-PO$_4^{3-}$ [ref.31]	55 °C, 1 atm O$_2$, 24 h, visible light	72
5	**Au/ZrO$_2$ in the present study**	**45 °C, 1 atm O$_2$, 24 h, NaOH**	**99**

[a] Reaction conditions: reaction temperature, pressure, reaction time, base.

Very recently, we developed a new methodology to use recyclable heterogeneous photocatalysts of gold-palladium alloy nanoparticles on a phosphate-modified hydrotalcite support (Au-Pd/HT-PO$_4^{3-}$) and molecular oxygen as a benign oxidant to drive the esterification of various primary aliphatic alcohols efficiently to esters at mild conditions. (1 atm O$_2$, 55 °C) [31]. In our point of view, an ideal oxidative catalytic process which could achieve higher activity and selectivity by a readily recyclable catalyst under atmospheric pressure of O$_2$ and at mild temperature is still highly desirable and of great interest.

In the present study, we describe that supported Au NPs on ZrO$_2$ could be used as an efficient catalyst for the self-esterification of aliphatic alcohols to corresponding esters under mild conditions (Table 1, entry 5). We prepared a series of supported AuNPs catalysts with various Au contents. The AuNPs catalysts were found to be efficient for the catalytic reaction with excellent yield and selectivity under mild reaction conditions. For example, the esterification of 1-octanol to octyl octanoate could be proceeded efficiently at 45 °C in atmospheric O$_2$, giving >99% yield and

selectivity. The heterogeneous Au NP catalyst could be reused for several runs without significant activity loss. Mechanistic and infrared emission spectroscopy (IES) studies were also conducted to clarify the reaction pathway in the reaction process. Evidently, an efficient and potential catalytic protocol is described and the results offer an alternative route to produce aliphatic esters.

2. Experimental

2.1. Preparation of catalysts

2.1.1 Chemicals

Zirconium (IV) oxide (ZrO_2, <100 nm particle size, TEM), gold(III) chloride trihydrate ($HAuCl_4 \cdot 3H_2O$, ≥99.9% trace metal basis), sodium borohydride, powder ($NaBH_4$, ≥98.0 %), and α,α,α-trifluorotoluene (anhydrous, 99 %) were purchased from Sigma-Aldrich (unless otherwise noted) and used as received without further purification. The water used in all experiments was prepared by being passed through an ultra-purification system.

2.1.2 Catalyst preparation

The Au NPs (Au supported on ZrO_2) were prepared by the impregnation-reduction method. For example, 3 wt% Au/ZrO_2 catalyst were prepared by the following procedure: ZrO_2 powder (2.0 g) was dispersed into a $HAuCl_4$ (30.4 mL, 0.01 M) aqueous solution under magnetic stirring at room temperature. A lysine (16 mL, 0.1 M) aqueous solution was then added to the mixture while it was vigorously stirred for 30 min, and the pH value was determined to be 8−9. Then, 6 mL of freshly prepared aqueous $NaBH_4$ (0.35 M) solution was added dropwise over 20 min. The mixture was aged for 24 h, and then the solid was separated by centrifugation, washed with water (three times) and ethanol (once), and dried at 60 °C in a vacuum oven for 24 h. The dried powder was used directly as a catalyst. AuNPs (0.5 ~ 5.0 wt%) were prepared

via a similar method but using different quantities of $HAuCl_4$ aqueous solutions, lysine aqueous solution and aqueous $NaBH_4$ solution.

2.2 Catalytic activity test

The reaction was conducted in a 10 mL Pyrex glass tube with a magnetic stirrer and placed in oil bath which could control the reaction temperature. The catalytic esterification of 1-octanol to octyl octanoate was used as the model reaction. Typically, Au/ZrO_2 catalyst (50 mg), NaOH (0.25 mmol) and 1-octanol (0.2 mmol) were added into 2 mL α,α,α-trifluorotoluene. The reaction tube was placed in an oil bath with magnetic stirring at 45 °C under O_2 atmosphere for 24 h. After reaction, aliquot (0.5 mL) was collected and filtered through a Millipore filter (pore size 0.45 mm) to remove the catalyst particles. The liquid-phase products were analysed and identified by gas chromatography mass spectrometer (GC-MS) including an Agilent HP5977A mass spectrometer attached to an Agilent 7890B gas chromatograph with a HP-5 column. Catalysts recycle experiment: after each reaction cycle, the solvent, substrate and products were removed by centrifugation; the separated catalyst was washed thoroughly with acetone three times, followed by centrifugal separation (5000 rpm, 10 min) and drying at 60 °C for 10 h. The resultant sample was used for recycle.

2.3 Characterization

The particle size and morphology of the catalysts was carried out on a JEOL 2100 transmission electron microscopy (TEM) with an accelerating voltage of 200 kV. X-ray diffraction (XRD) patterns of the samples were collected by using a Philips PANalytical X'Pert PRO diffractometer with Cu Kα radiation (λ=1.5418 Å) at a fixed power source (40 kV and 40 mA). electron microscope (SEM) imaging, elemental mapping, and Energy Dispersive X-Ray Spectroscopy (EDS) were performed using a ZEISS Sigma SEM at accelerating voltages of 20 kV. Nitrogen physisorption

isotherms were measured at -196 °C on the Tristar II 3020. Before the test, the samples were dried under vacuum condition at 120 °C for 24 h. The specific surface area was calculated by the Brunauer-Emmett-Teller (BET) method from the data in a P/P_0 range between 0.01 and 1.0. X-ray photoelectron spectroscopy (XPS) data was acquired using a Kratos Axis ULTRA X-ray Photoelectron Spectrometer incorporating a 165 mm hemispherical electron energy analyser. The incident radiation was Monochromatic Al Kα X-rays (1486.6 eV) at 225 W (15 kV, 15 ma). Narrow high-resolution scans were run with 0.05 eV steps and 250 ms dwell time. Base pressure in the analysis chamber was 1.0×10^{-9} torr and during sample analysis 1.0×10^{-8} torr. Peak fitting of the high-resolution data was carried out using the CasaXPS software. The infrared emission spectroscopy (IES) measurements on a Digilab FTS-60A spectrometer equipped with a TGS detector, which was modified by replacing the IR source with an emission cell.

3. **Results and discussion**

3.1 The structure of catalysts

In this study, we prepared a series of Au NP catalysts supported on zirconia (ZrO_2) with various Au loading (0.5 wt%, 1.5 wt%, 3.0 wt% and 5.0 wt%) by the impregnation-reduction method [32-35]. The ZrO_2 enables the uniform distribution of Au NPs on the solid support surface, and the readily recycling of the catalysts after reaction. The as-prepared catalysts were characterized with various techniques to confirm the composition and morphology. TEM images in Figure 1 provide direct information of the size, shape and distribution of Au NPs with different content on the ZrO_2 support. We can see that Au NPs distribute evenly on the ZrO_2 support surface, and no obvious agglomerations were observed for the Au NPs prepared via this impregnation-reduction method. The mean sizes of the particles are ranging from 4.31 to 5.63 nm for catalysts with various Au loading. Thus this method provides a

simply process to prepare small Au NPs with average size around 5 nm, in the range of Au loading from 0.5 to 5.0 wt%.
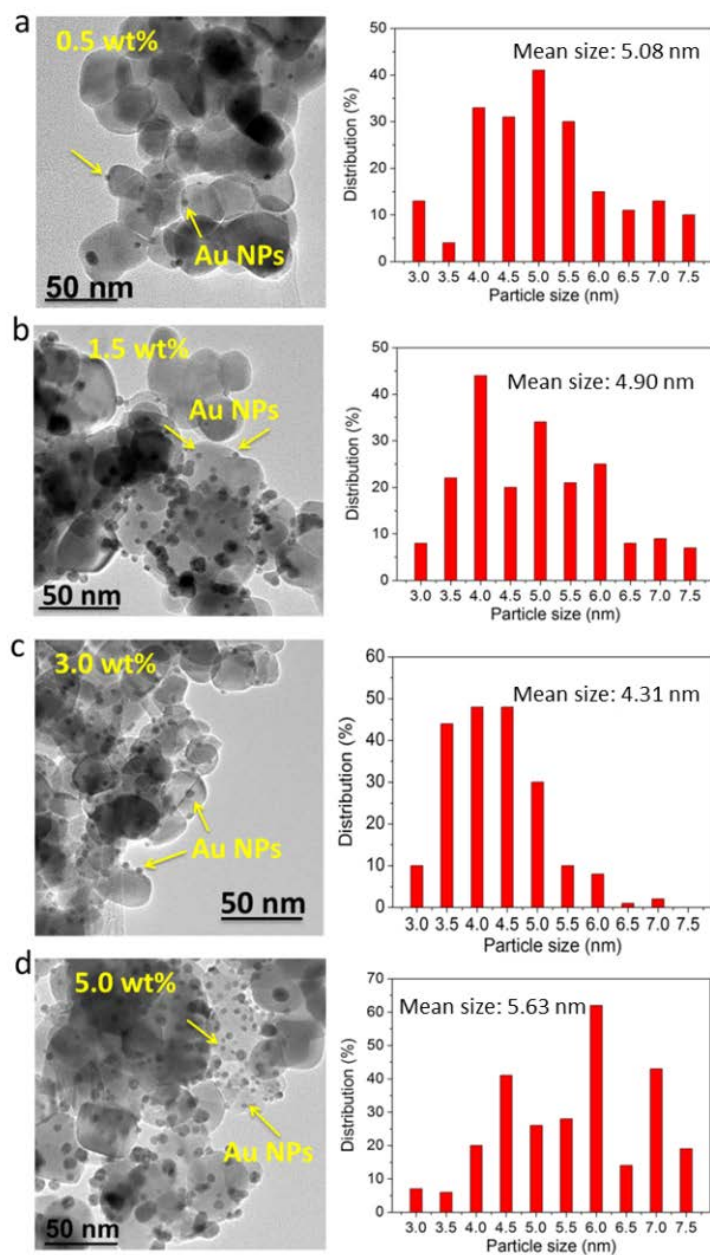

Figure 1. TEM images of the catalysts with different Au loading and the relevant Au particle size distribution. (a) Au/ZrO$_2$ (0.5 wt%), (b) Au/ZrO$_2$ (1.5 wt%), (c) Au/ZrO$_2$ (3.0 wt%) and (d) Au/ZrO$_2$ (5.0 wt%). The particle size distribution were calculated by measuring >200 isolate particles in the images of the corresponding catalyst.

The X-Ray diffraction (XRD) shows the patterns of the catalysts with different Au contents on ZrO_2 (Figure S1, SI). All diffraction peaks can be indexed to a monoclinic structure of the ZrO_2 crystal (JCPDS, no. 65-2357), no reflection peaks of Au were observed by the XRD patterns, because the metal content is low and the metal diffraction peaks may interfere with the diffraction peaks of ZrO_2; this result suggests that the detection of metal NP signals in XRD patterns is also closely related to the supporting materials.

The Brauner−Emmet−Teller (BET) specific surface areas of the samples were derived from N_2 physical sorption data of the samples using the BET method, which are similar to that of the ZrO_2 support (approximately 33 m^2/g). The ZrO_2 support has a moderate specific surface area, and loading with 3 wt% Au does not cause significant change in the overall specific surface area of sample. The isotherm exhibits an H_3-type hysteresis at high relative pressure (Figure 2), which is typical for aggregates of plate-like particles [36], the enclosure of adsorption/desorption branches were observed for all the samples at relatively high p/p_0 about 0.85, which could be attributed to the presence of large mesoporous structure and/or some macropores. This kind of hysteresis is typical for the presence of open large pores, which allow easy diffusion of the reactants through the materials. This offered sufficient interfaces to facilitate the effective contact between reactants and the catalyst.
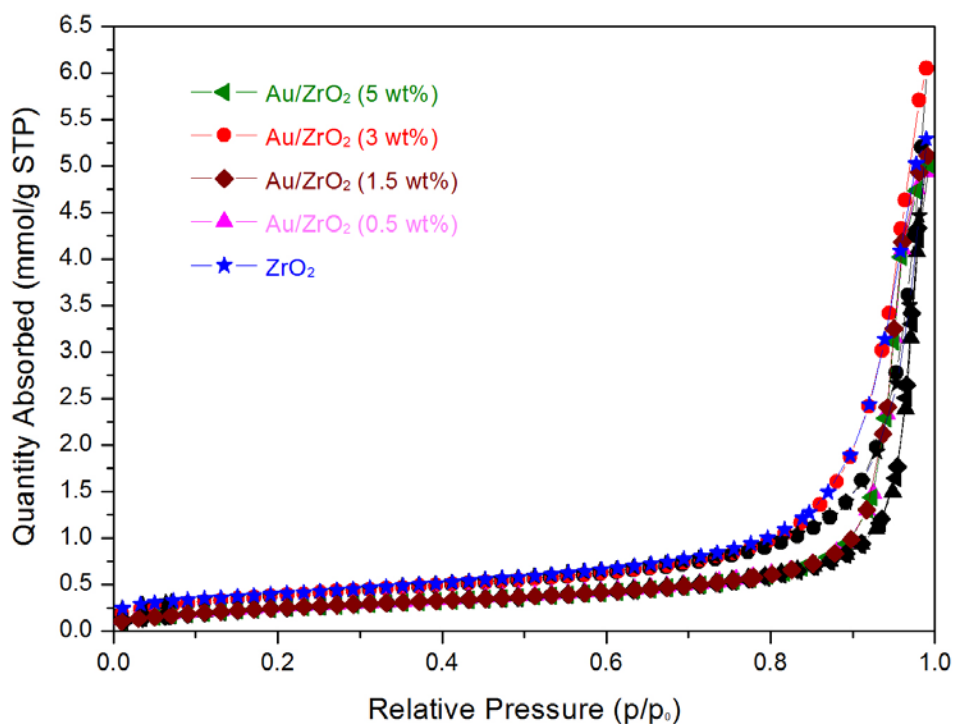
Figure 2. N$_2$ adsorption (colored symbol)/desorption (black symbol) isotherms of the catalysts and ZrO$_2$ support.

3.2 Catalytic activity

We tested the catalytic activity of the Au/ZrO$_2$ catalysts with various Au loadings using the oxidative esterification of 1-octanol as the model reaction. As show in Table 2, all the Au catalysts exhibit excellent conversion and selectivity for the esterification reaction, and among them the Au/ZrO$_2$ (3.0 wt%) catalyst gave almost full conversion and product selectivity. Compared with those reported process for the catalytic esterification of aliphatic alcohols typically conducted under much higher temperatures and pressures [28-30], our heterogeneous Au NP catalytic system could be controlled under mild reaction conditions more efficiently (1 atm O$_2$, 45 °C), which exhibits apparent advantages in the viewpoint from green chemical synthesis. It is noteworthy that when the Au loading was only 0.5 wt%, the catalyst could gave very high turnover number (TON) of 131, this result suggests that it is

possible to achieve high catalytic efficiency even with very a low Au loading. Blank experiment under otherwise identical reaction conditions but without Au NPs was also conducted and was catalytically inactive in this transformation. Further increasing the Au content to 5.0 wt% gave lower conversion and much lower TON. As shown in the TEM data that there is slight increase in the particle size for those catalysts gave relevant lower catalytic activity. The results revealed that Au NPs catalysts with larger particle size exhibited lower activity and selectivity, and the catalyst with 3.0 wt% Au exhibited the best performance in our catalytic system. Thus it is possible to further adjust the catalytic activity and the product selectivity by optimizing the particle sizes, shape and distribution of Au NPs.

Table 2. Activity test and catalyst screening of different Au content for oxidative esterification of 1-octanol.[a]
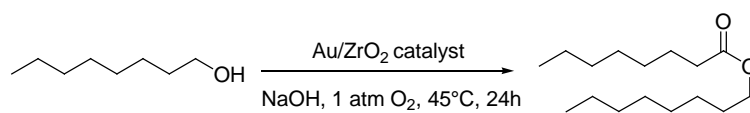
Entry	Catalyst	Conv. (%)	Select.(%)	Yield (%)	TON[b]
1	Au/ZrO$_2$ (0.5 wt%)	86	97	83	131
2	Au/ZrO$_2$ (1.5 wt%)	96	99	95	50
3	Au/ZrO$_2$ (3.0 wt%)	100	99	99	26
4	Au/ZrO$_2$ (5.0 wt%)	91	99	90	14
5	ZrO$_2$	0	0	0	0

[a] Reaction conditions: Au/ZrO$_2$ catalyst 50 mg, reactant 0.2 mmol, NaOH 0.25 mmol, solvent α,α,α-trifluorotoluene 2 mL, 1 atm O$_2$, reaction temperature 45 °C, reaction time 24 h. The conversions and selectivity were calculated from the product formed and the reactant converted measured by gas chromatography mass spectrometry (GC-MS). [b] TON was calculated as $n_{product}/n_{NPs}$, where $n_{product}$ and n_{NPs} were the mole number of the product formed and the active metal, respectively.

As the Au/ZrO$_2$ (3.0 wt%) catalyst showing the optimal catalytic activity, we further investigated its morphology details by high resolution TEM (HR-TEM) and Scanning electron microscopy (SEM) (Figure 3). The Au NPs are spherical and the lattice fringe spacing of 0.23 nm corresponds to the interplanar distance of (111) planes in the Au lattice (Figure 3b) [33,37]. To investigate the elemental composition in the Au NP catalyst, energy-dispersive X-ray spectroscopy (EDX) elemental mappings of the Au/ZrO$_2$ (3.0 wt%) catalyst were performed (Figure 3c). EDX elemental mapping of the SEM image shows that all the components are homogeneously distributed throughout the sample. The percentages of Zr, O, and Au elements in the catalysts were also analysed from the EDX spectrum (Figure 3d), the Zr, O, and Au are matched with the initial experimental design. X-ray photoelectron spectra (XPS) of the samples confirm that gold exists in the metallic state on ZrO$_2$ supports (Figure 3e). The binding energies of Au 4f7/2 and Au 4f5/2 electrons are 84.1 and 87.8 eV, respectively, which are identical to the bulk of gold metal [33,38,39].
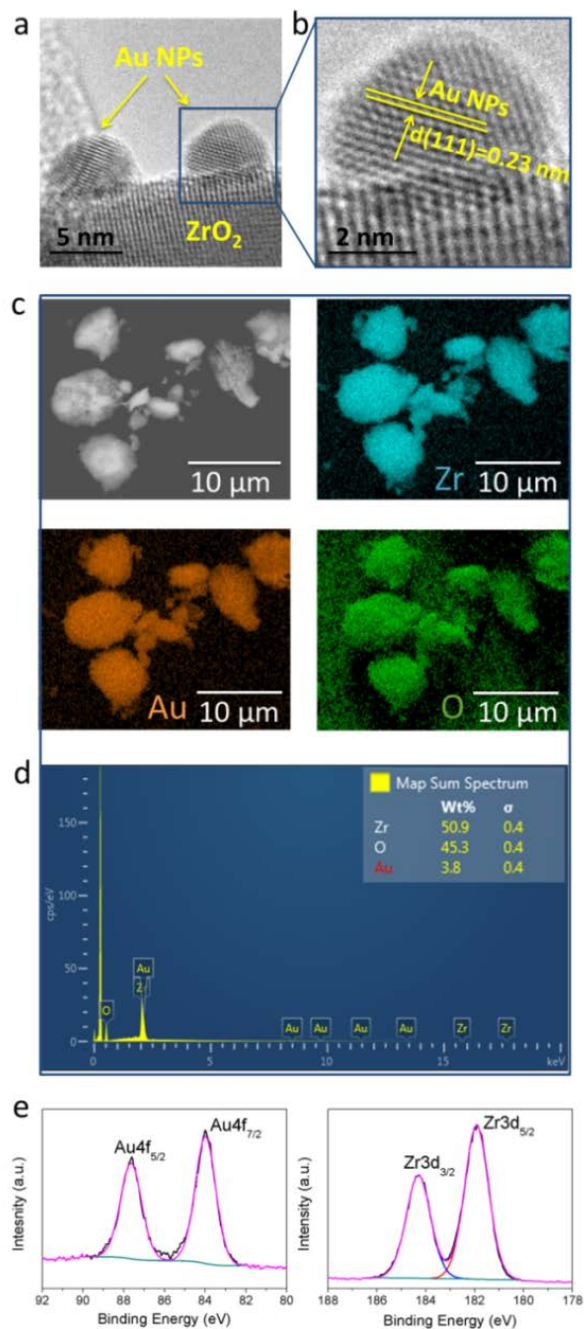
Figure 3. (a) HR-TEM image of the Au/ZrO$_2$ (3.0 wt%). (b) HR-TEM image of an typical Au particle indicated in the square in (a). (c) SEM image of Au/ZrO$_2$ (3.0 wt%) sample, the corresponding EDX mapping of Zr, Au, O elements, and (d) the EDX spectrum. (e) XPS profile of Au and Zr species in the Au/ZrO$_2$ (3.0 wt%) catalyst.

3.3 Influence of base and solvent

The influence of several critical reaction conditions in the oxidative esterification of 1-octanol, such as solvents and bases, was investigated using the Au/ZrO$_2$ (3 wt%) catalyst. To

understand the effect of various bases on the performance of the catalytic system, we employed various base additives in the model reaction and the results are listed in Table 3. The reaction did not show any activity without base additive, which means that base additives are essential for this catalytic system (entry 1). We also found that weak base additives such as Na_2HPO_4, NaH_2PO_4, K_3PO_4 and K_2CO_3 are not able to drive the catalytic reaction, while only Na_3PO_4 gave poor conversion (23%) and ester selectivity (52%) (entries 2-6). Strong bases such as KOH and NaOH can promote the reaction efficiently, achieving high ester selectivity (99%) (entries 7 and 8), and when using NaOH as the base the catalytic reaction exhibited the best performance.

Table 3. Activity test of different base additives for the oxidative esterification of 1-octanol using the Au/ZrO_2 (3.0 wt%) catalyst.[a]
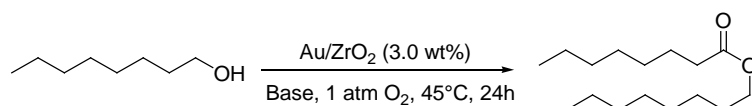
Entry	Additives	Conv. (%)	Select. (%)	Yield (%)
1	-	0	0	0
2	Na_3PO_4	23	52	12
3	Na_2HPO_4	0	0	0
4	NaH_2PO_4	0	0	0
5	K_3PO_4	0	0	0
6	K_2CO_3	0	0	0
7	KOH	77	99	76
8	NaOH	100	99	99

[a] Reaction conditions: Au/ZrO_2 (3.0 wt%) catalyst 50 mg, reactant 0.2 mmol, base additive 0.25 mmol, solvent α,α,α-trifluorotoluene 2 mL, 1 atm O_2, reaction temperature 45 °C,

reaction time 24 h. The conversions and selectivity were calculated from the product formed and the reactant converted measured by GC-MS.

Moreover, several commonly used solvents were also examined for the reaction with other conditions were maintained unchanged (Table 4). It is obviously that α,α,α-trifluorotoluene exhibited the best performance (entry 1). The polar solvents such as acetonitrile and isopropanol afforded low yields of ester (entries 4 and 5). In contract much higher yield was observed in the nonpolar solvent (entries 2 and 3). The preferable nonpolar solvent facilitates the reaction more efficiently probably due to the better solubility for aliphatic alcohol reactant.

Table 4. The influence of solvent for the oxidative esterification of 1-octanol using Au/ZrO_2 (3.0 wt%) catalyst.[a]

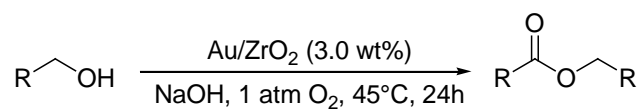| Entry	Solvent	Conv. (%)	Select. (%)	Yield (%)
1	α,α,α-trifluorotoluene	100	99	99
2	n-heptane	89	99	88
3	toluene	92	99	92
4	acetonitrile	56	98	55
5	isopropanol	0	0	0

[a] Reaction conditions: Au/ZrO_2 (3.0 wt%) catalyst 50 mg, reactant 0.2 mmol, NaOH 0.25 mmol, solvent 2 mL, 1 atm O_2, reaction temperature 45 °C. The conversions and selectivity were calculated from the product formed and the reactant converted measured by GC-MS.
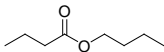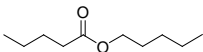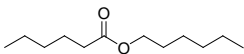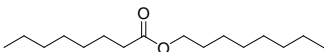
3.4 Esterification of various aliphatic alcohols

With the optimized conditions in hand, the catalytic performance of Au/ZrO_2 (3.0 wt%) catalyst for various alcohol substrates was investigated. All the reactions were carried out at 45 °C in 1 atm O_2 using NaOH as the base and solvent α,α,α-trifluorotoluene as the reaction medium. The direct oxidative esterification of a series of aliphatic alcohols with various

carbon chain lengths were investigated and the results are summarized in Table 5. Excellent

yields of the corresponding esters were achieved for most of the examples studied with high

selectivities (>99%). Among them, oxidative esterification of 1-nonane and 1-butanol

exhibited relative moderate yields (entries 1 and 6). These results demonstrate that the

supported Au NP catalyst can efficiently convert various aliphatic alcohols to the

corresponding ester derivatives under relevant mild reaction conditions.

Table 5. The direct oxidative esterification of various aliphatic alcohols using Au/ZrO_2 (3.0

wt%) catalyst.[a]

Entry	Ester	Yield (%)[b]	TON[c]	TOF[d] (h^{-1})
1		68	18	0.75
2		93	24	1.00
3		>99	26	1.08
4		>99	26	1.08
5		>99	26	1.08
6		88	23	0.96
7		>99	26	1.08
8		>99	26	1.08

[a] Reaction conditions: Au/ZrO_2 (3.0 wt%) catalyst 50 mg, reactant 0.2 mmol, NaOH 0.25

mmol, solvent α,α,α-trifluorotoluene 2 mL, 1 atm O_2, reaction temperature 45 °C, reaction

time 24 h. [b] The yields were calculated from the product formed and the reactant converted
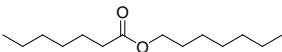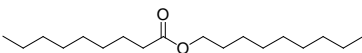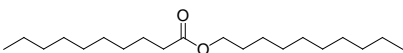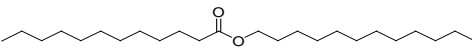
measured by GC-MS. [c] TON was calculated as $n_{product}/n_{NPs}$, where $n_{product}$ and n_{NPs} were the mole number of the product formed and the active metal, respectively. [d] TOF=TON/reaction time.
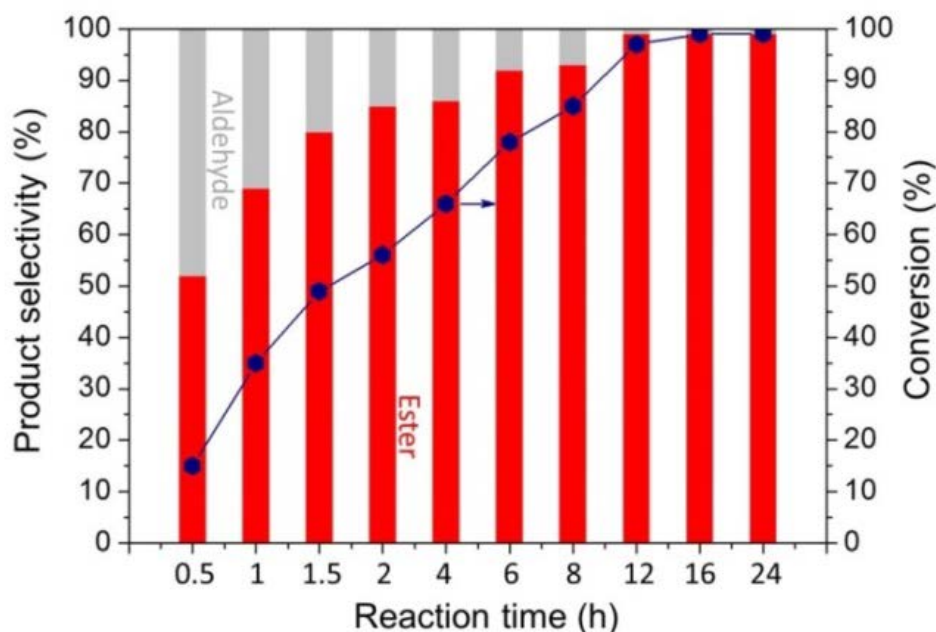

Figure 4. The time course for the catalytic activities [reaction conversion and product selectivity (red for ester, gray for aldehyde)] of the oxidative esterification of 1-octanol. Reaction conditions: Au/ZrO$_2$ (3.0 wt%) 50 mg, 1-octanol 0.2 mmol, NaOH 0.25 mmol, α,α,α-trifluorotoluene 2 mL, 1 atm O$_2$, reaction temperature 45 °C, reaction time 24 h.

3.5 Reaction pathway

To gain insight into the mechanism of the reaction process, we studied the evolution of the products during the time course of the oxidative esterification of 1-octanol using Au/ZrO$_2$ (3.0 wt%) catalyst (Figure 4). It can be seen that the conversion of the reaction increased steadily during the time course, and the aldehyde is the main intermediate during the reaction course. The selectivity to ester increased with the prolonging of reaction time. This suggests that the alcohol was firstly oxidized to corresponding aldehyde during process and then the aldehyde further reacts with rest of alcohol molecule to achieve the esterification.

To further explore the mechanism of the reaction process, we investigate whether alcohol is essential for esterification once aldehyde produced. In this regard, 1-ocatanol was replaced with 1-octanal in the beginning of reaction process but maintained other conditions unchanged. We found that after 24 h reaction, no ester product was detected (Table 6, entry 1). Whereas, when using both 1-octanol and 1-octanal as the starting material, the reaction could proceed smoothly to obtain the corresponding ester.

Table 6. The mechanistic study of alcohol and aldehyde in the esterification process.[a]

Entry	Reactant	Conv. (%)	Select. (%)	Yield (%)
1	1-octanal	0	0	0
2[b]	1-octanol+ 1-octanal	87	87	76

[a] Reaction conditions: Au/ZrO$_2$ (3.0 wt%) catalyst 50 mg, reactant 0.2 mmol, NaOH 0.25 mmol, solvent α,α,α-trifluorotoluene 2 mL, 1 atm O$_2$, reaction temperature 45 °C, reaction time 24 h. The conversions and selectivity were calculated from the product formed and the reactant converted measured by GC-MS. [b] 0.1 mmol of reactant respectively.

A tentative mechanism for the direct oxidative esterification of aliphatic alcohols is proposed in Scheme 1 on the basis of our experimental observation and the literature [31,40-45]. Initially, the reactant adsorbed on the Au NP surface due to the strong interactions. The selective oxidation of the primary alcohols in the presence of Au NPs proceeds to form aldehydes (step 1). The presence of NaOH is needed for the deprotonation of alcohols, making them more susceptible to oxidation to aldehyde [46]. Then, the condensation reaction between aldehyde and alcohol takes place, leading to the formation of hemiacetal species (step 2) [28,29,31,47]. NaOH favors the formation of hemiacetal, which could lead to higher electivity of esters [6]. The ester products are directly formed by the direct oxidation of hemiacetals (step 3). Au NP catalyst may facilitate both oxidation and hemiacetal formation

in a single step under mild conditions, which could significantly promote the oxidative esterification [47].
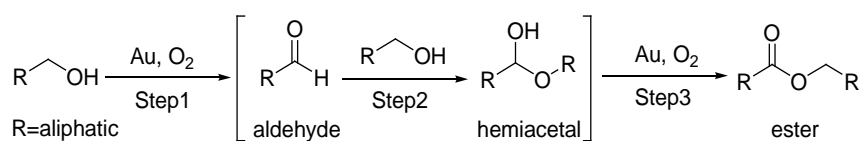
Scheme 1. Possible reaction pathways for the esterification over Au/ZrO$_2$ catalyst in the present study.

To confirm the interaction of the reactant with the surface of the catalyst, we conducted the infrared emission spectroscopy (IES) analysis with the Au/ZrO$_2$ (3.0 wt%) catalyst and 1-pentanol as the reactant (Figure 5). We can clearly see the presence of peaks attributed to the alkane C-H stretching below 3000 cm-1 for the Au catalyst adsorbed with 1-pentanol. The absorbance peak became weak with the elevating of the temperature, and disappeared at 400 °C (Figure 5a). For comparison, we also tested the sample using ZrO$_2$ support without Au NPs, the sample exhibited much weaker absorbance than the sample with Au NPs (Figure 5b). This result suggested that Au NPs can strongly adsorb the reactant molecule on their surface, which facilitates the reaction efficiently.
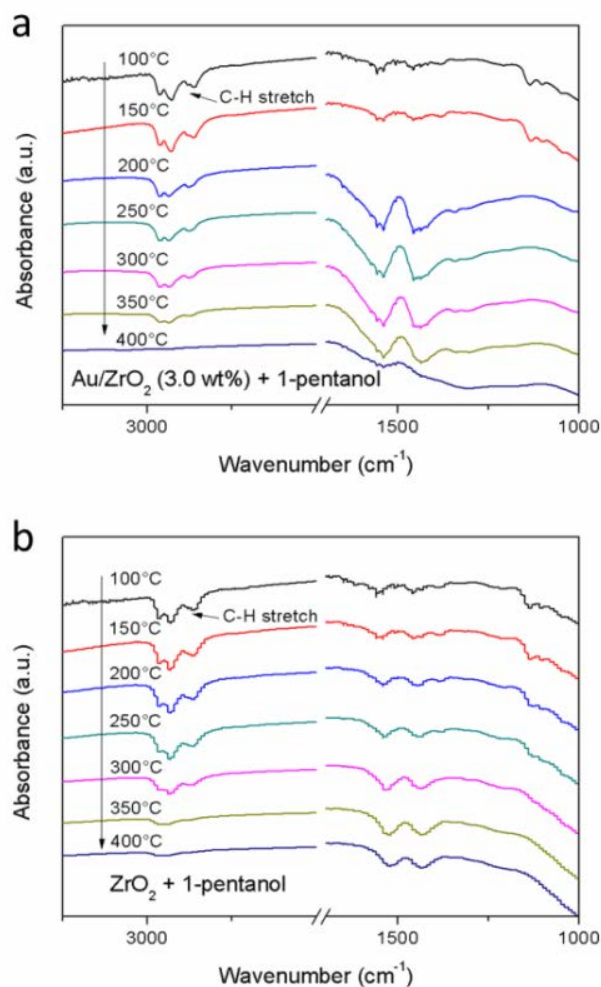
Figure 5. (a) IES spectra of 1-pentanol adsorbed on Au/ZrO$_2$ (3.0 wt%) catalyst. (b) IES spectra of 1-pentanol adsorbed on ZrO$_2$ support.

3.6 Recycle of catalyst

For practical applications of heterogeneous catalyst, the reusability of the catalyst is an important factor, particularly when precious metals are used. Au/ZrO$_2$ (3.0 wt%) catalyst was used for five consecutive runs of oxidative esterification of 1-octanol to demonstrate the recyclability of the catalyst. The reaction conditions were kept identical for each run and after each reaction cycle, the catalyst was separated by centrifugation, washed thoroughly with acetone three times, and then dried for subsequent reactions. As shown in Figure 6, the catalyst was reused for five cycles without significant loss of activity. From the typical TEM

image of the catalyst after being recycled (Figure 6b), the Au NPs still distribute evenly on the surface of ZrO$_2$ support, and no obvious agglomeration was observed.
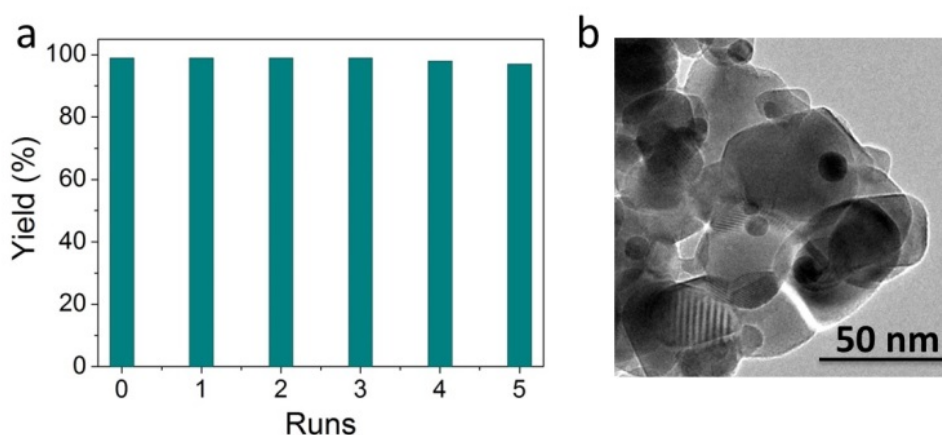

Figure 6. (a) The catalytic activity of the Au/ZrO$_2$ (3.0 wt%) catalyst after being recycled five times. (b) Representative TEM image of the Au/ZrO$_2$ (3.0 wt%) catalyst after being recycled.

4. **Conclusions**

In conclusion, we demonstrated that supported Au NPs can efficiently drive self-esterification of primary aliphatic alcohols to corresponding esters directly, achieving excellent activity and selectivity under mild reaction conditions. The present catalytic system can be applied in catalyse various aliphatic alcohols into the corresponding esters in high yields. Au NPs catalyst can be efficiently recycled after reaction and reused without significantly losing activity, which showing its great heterogeneous advantage. The knowledge acquired in this study may inspire further studies on new efficient catalytic system for a wide range of organic syntheses using supported Au NP catalysts. Since these long aliphatic esters are high-value chemicals, finding use as surfactants, lubricants and emulsifiers etc. These results may open the door to new green processes for producing high-value alkyl esters.

Acknowledgements

References list

1. B.R. Davis, P.J. Garratt, Comprehensive Organic Synthesis, ed. Trost, B. M.; Fleming, I. Pergamon Press, Oxford, 1991, vol. 2, p. 799.

2. J. March, Advanced Organic Chemistry, Wiley, New York, 1985.

3. R.C. Larock, in Comprehensive Organic Transformations, VHC, New York, 1989, p. 966.

4. B. Zugic, S. Karakalos, K.J. Stowers, M.M. Biener, J. Biener, R.J. Madix, C. M. Friend, ACS Catal. 6 (2016) 1833-1839.

5. L.C. Wang, K.J. Stowers, B. Zugic, M.M. Biener, J. Biener, C.M. Friend, R.J. Madix, Catal. Sci. Technol. 5 (2015) 1299-1306.

6. Y.C. Li, L. Wang, R.Y. Yan, J.X. Han, S.J. Zhang, Catal. Sci. Technol. 5 (2015) 3682-3692.

7. W. Zhong, H.L. Liu, C.H. Bai, S.J. Liao, Y.W. Li, ACS Catal. 5 (2015) 1850-1856.

8. W. Riemenschneider, M.H. Bolt, "Esters, Organic" Ullmann's Encyclopedia of Industrial Chemistry, Wiley-VCH, Weinheim, 2005.

9. J. Otera, Esterification: Methods, Reactions, and Applications; Wiley-VCH: Weinheim, 2003.

10. R.C. Larock, Comprehensive Organic Transformations: A Guide to Functional Group Preparations, 2nd ed.; Wiley-VCH: New York, 1999.

11. J. Mulzer, in Comprehensive Organic Synthesis, Vol. 6, ed. B.M. Trost, I. Fleming, Pergamon Press, Oxford, 1991, p. 324.

12. B. Xu, X. Liu, J. Haubrich, R.J. Madix, C.M. Friend, Angew. Chem. Int. Ed. 48 (2009) 4206-4209.

13. S. Arita, T. Koike, Y. Kayaki, T. Ikariya, Chem. Asian J. 3 (2008) 1479-1485.

14. A. Abad, P. Concepción, A. Corma, H. Garc, Angew. Chem. Int. Ed. 44 (2005) 4066-4069.

15. J. Goldemberg, Science 315 (2007) 808-810.

16. C. Liu, J. Wang, L.K. Meng, Y. Deng, Y. Li, A.W. Lei, Angew. Chem. Int. Ed. 123 (2011) 5250-5254.

17. S. Gowrisankar, H. Neumann, M. Beller, Angew. Chem. Int. Ed. 50 (2011) 5139-5143.

18. J. Zhang, G. Leitus, Y. Ben-David, D. Milstein, J. Am. Chem. Soc. 127 (2005) 10840-10841.

19. C. Gunanathan, J.W.S. Linda, D. Milstein, J. Am. Chem. Soc. 131 (2009) 3146-3147.

20. A. Abramovich, H. Toledo, E. Pisarevsky, A.M. Szpilman, Synlett 23 (2012) 2261-2265.

21. Y. Tamura, Y. Yamada, K. Inoue, Y. Yamamoto, Z. Yoshida, J. Org. Chem. 48 (1983) 1286-1292.

22. K.M. Kosuda, A. Wittstock, C.M. Friend, M. Bäumer, Angew. Chem. Int. Ed. 51 (2012) 1698-1701.

23. G.T. Whiting, S.A. Kondrat, C. Hammond, N. Dimitratos, Q. He, D.J. Morgan, N.F. Dummer, J.K. Bartley, C.J. Kiely, S.H. Taylor, G.J. Hutchings, ACS Catal. 5 (2015) 637-644.

24. P.P.M. Schleker, R. Honeker, J. Klankermayer, W. Leitner, ChemCatChem 5 (2013) 1762-1764.

25. M. Nielsen, H. Junge, A. Kammer, M. Beller, Phys. Chem. Chem. Phys. 12 (2010) 1741-1749.

26. A. Izumi, Y. Obora, S. Sakaguchi, Y. Ishii, Tetrahedron Lett. 47 (2006) 9199-9201.

27. J. Zhang, G. Leitus, Y. Ben-David, D. Milstein, Angew. Chem. Int. Ed. 45 (2006) 1113-1115.

28. T. Ishida, Y. Ogihara, H. Ohashi, T. Akita, T. Honma, H. Oji, M. Haruta, ChemSusChem 5 (2012) 2243-2248.

29. R.V. Jagadeesh, H. Junge, M.M. Pohl, J. Radnik, A. Brückner, M. Beller, J. Am. Chem. Soc. 135 (2013) 10776-10782.

30. S. K. Moromi, S.M.A.H. Siddiki, M.A. Ali, K. Kona, K. Shimizu, Catal. Sci. Technol. 4 (2014) 3631-3635.

31. Q. Xiao, Z. Liu, A. Bo, S. Zavahir, S. Sarina, S. Bottle, J.D. Riches, H.Y. Zhu, J. Am. Chem. Soc. 137 (2015) 1956-1966.

32. S. Sarina, H.Y. Zhu, E. Jaatinen, Q. Xiao, H.W. Liu, J.F. Jia, C. Chen, J. Zhao, J. Am. Chem. Soc. 135 (2013) 5793-5801.

33. Y.L. Zhang, Q. Xiao, Y.S. Bao, Y.J. Zhang, S. Bottle, S. Sarina, B. Zhaorigetu, H.Y. Zhu, J. Phys. Chem. C. 118 (2014) 19062-19069.

34. X. Chen, H.Y. Zhu, J.C. Zhao, Z.F. Zheng, X.P. Gao, Angew. Chem. Int. Ed. 47 (2008) 5353-5356.

35. H.Y. Zhu, X. Chen, Z.F. Zheng, X.B. Ke, E. Jaatinen, J.C. Zhao, C. Guo, T.F. Xie, D.J. Wang, Chem. Commun. (2009) 7524-7526.

36. D. Meloni, R. Monaci, V. Solinas, A. Auroux, E. Dumitriu, Appl. Catal. A: Gen. 350 (2008) 86-95.

37. Y. Li, H. Wang, Q.Y. Feng, G. Zhou, Z.S. Wang, Energy Environ. Sci. 6 (2013) 2156-2165.

38. O.M. Khatri, K. Murase, H. Sugimura, Langmuir 24 (2008) 3787-3793.

39. X.G. Zhang, X.B. Ke, H.Y. Zhu, Chem. Eur. J. 18 (2012) 8048-8056.

40. X.F. Wu, C. Darcel, Eur. J. Org. Chem. (2009) 1144-1147.

41. K. Suzuki, T. Yamaguchi, K. Matsushita, C. Iitsuka, J. Miura, T. Akaogi, H. Ishida, ACS Catal. 3 (2013) 1845-1849.

Chapter 4:

Conclusions and Future Work

Conclusions:

In this thesis, Pd NPs and Au NPs catalysts have been developed and used for selective organic reactions under visible light irradiation and in tehrmal condition, respectively:

In Chapter 2, a effective and reusable heterogeneous Pd NPs supported on ZrO_2 catalyst exhibit high activity and product selectivity for the Heck reactions. The Pd NP photocatalyst shows excellent activity and high selectivity of both isomeric cross-coupling product under light irradiation and moderate temperature. Tuning light intensity and wavelength can affect catalytic activity and modulate selectivity of cis- or trans-isomer. This study provides a general guiding principle for determing the applicability of Pd photocatalysts as well as a inspiration for optimizing suitable reaction system catalzyed by Pd photocatalyst in other organic tranfomartion process.

In Chapter 3, we conducted Au NP catalyst to an thermal chemical process, and the Au NPs can drive self-esterification of aliphatic alcohols to esters under moderate condition in atmospheric O_2. The feasaible catalytic reaction pathway was proposd, and it points out the alcohol will first transformed to aldehyde and then the condensation occured between aldehyde and alohol, thus produced ester.

In conclusion, the catalytic system destribed here may present a new strategy towards the development of new heterogeneous catalysts, and also contribute to understand the development of photocatalytic systems for more complex organic reactions.

Future Work:

1. As we know, there are many transition metals besides Pd which are catalytically active and widely used in photocatalytic reactions. The extent of other transition metals should also be devised as supported photocatalysts in our future work. Furthermore, combination of Pd with plasmonic-metal (Au, Ag, Cu) should be designed as new of supported alloy NP photocatalysts. They can provide active sites in photocatalytic reactions. Plasmonic has strong absorption in visible light due to the LSRP effect and it maintains stable in air. Combining the two kinds of metals, the more stable and active alloy NP photocatalysts could be developed to drive more complicated organic syntheses.

2. The light absorption of both the plasmonic and nonplasmonic nanostuctures is tuneable by altering particle geometry such as size, shape and composition, which provides us a possible concept to design nanosturctures that can efficiently absorb visible light by manipulating the properties. In additional, different supports also play a key role in photocatalysis process by their different absoprtion mechnism. We will focus the structure improvement not only on the metal NPs but also the vatious supports.

3. The ultimate aim of our research is to utilise solar energy to enhance organic reaction rate and the selectivty of specific product. Therefore, figure out the impact factors of this process is of great concern and should be investigated in detail. The affinity of the catalysts to the reactant is one of the significant factora. For our reported work, we use supported metal NPs as photocatalyst, therefore to change the affinity of support to the

reactant is another potential way to enhance product yield. In this case, the improvement of supports is an important direction to enhance the photocatalyzed reaction rate in our further study.